Aluminium alloys as structural material: A review of research

Evangelia Georgantzia[a,1], Michaela Gkantou[a] , George S. Kamaris[a]

[a] Department of Civil Engineering, Liverpool John Moores University, United Kingdom

ABSTRACT

Over the last few decades aluminium alloys have been increasingly used in the construction sector due to their favourable properties. Thereafter, many research projects have been carried out with the aim to obtain a more comprehensive understanding of their structural performance and develop accurate and reliable design formulae. The scope of this paper is to provide a comprehensive review of research by discussing the reported experimental, numerical and analytical work on structural aluminium alloys. The paper presents an overview of research studies on the mechanical properties of aluminium alloys under monotonic, cyclic and thermal loading conditions. Moreover, a considerable amount of experimental and numerical investigations focussing on the structural performance and design of aluminium columns, beams and beam-columns is reviewed. The performance of connections and composite aluminium-concrete members is also discussed. Comments on the suitability of the international design specifications to structural aluminium alloys are included. Within the review, knowledge gaps are identified and the corresponding research work to fill these gaps is recommended.

Keywords: aluminium alloys, structural response, experiments, numerical investigation, design guidelines

[1]Corresponding author: Evangelia Georgantzia
Email: E.Georgantzia @2019.ljmu.ac.uk

1 Introduction

The application of aluminium alloys as structural material has increased over the last years owing to their favourable properties: i.e. high strength-to-weight ratio, ease of fabrication, high degree of workability, considerable ductility, excellent thermal conductivity, high corrosion resistance and attractive appearance at their natural finish. For this reason, 25% of the global aluminium production is currently used in the construction sector [1]. Their ease of extrusion makes aluminium alloys a versatile structural material allowing the production of complex cross-sectional shapes, suitable for structures that cannot be developed from more conventional structural materials, such as concrete or steel. Their prominent corrosion resistance makes them well-suited for applications in marine environments without surface protection and with low maintenance cost. Their great durability allows for structures that can maintain their inherent properties even in large temperature variations [1]. Within the framework of sustainability and climate-change mitigation commitments, recent technological advances led to innovative aluminium structural systems that are more efficient from an environmental and economical point of view compared to steel and concrete. In particular, advances on the manufacturing process of aluminium alloys reduced the required energy more than 75% since 1995, lowering the industry's carbon footprint by almost 40% [2]. It has been also stated that "aluminum made in North America is more sustainable today than ever before" [2]. Further to the decrease in carbon dioxide emissions, structural aluminium alloys are 100% recyclable, thereby arguably winning the title of "green metal" [3].

The aforementioned advantageous features have contributed to increased usage of aluminium alloys in structural applications, where their application can allow for a reduction of the total structural weight. Typical structural aluminium applications along with brief information are presented in Figure 1. As with all structural materials, structural design codes are warranted for aluminium alloy structures. Currently there are four international design specifications for the structural design of aluminium alloys, as listed in Table 1.

Table 1: International Design Specifications for Aluminium Alloy Structures.

Standard ID	Standard Title [Description]
Chinese Standard: GB 50429-2007 [4]	Code for design of aluminium structures
European Committee for Standardization: BS EN 1999:2007 [5]	Design of aluminium structures
Australian/New Zealand Standard: AS/NZS 1664:1997 [6]	Aluminium structures
The Aluminum Association: AA 2020 [7]	Aluminum Design Manual

2003

St Mary Axe, London, UK
A curved and anodised aluminium skin was used to integrate the raking columns with the curved façade.

2004

The Sage Gateshead, Gateshead Quays, UK
Aluminium was used to support the glazing system.

2010

Ferrari World, Abu Dhabi, UAE
The largest aluminium roof in the world. A corrugated aluminium sheet was selected as roof material.

2004

Gaylord Texan Resort & Convention Center, Grapevine, Texas, USA
The roof is made of a glazed aluminium framework.

2012

The Crystal, London, UK
The roof is made from 100% recycled aluminium.

2012

The Iceberg Skating Palace, Sochi, Russia
Aluminium was one of the key materials used to the construction.

2019

Casablanca Finance City Tower, Casablanca, Morocco
The modular façade elements were made out from aluminium instead of concrete for cost reasons.

2013

The Co-operative Group, Manchester, UK
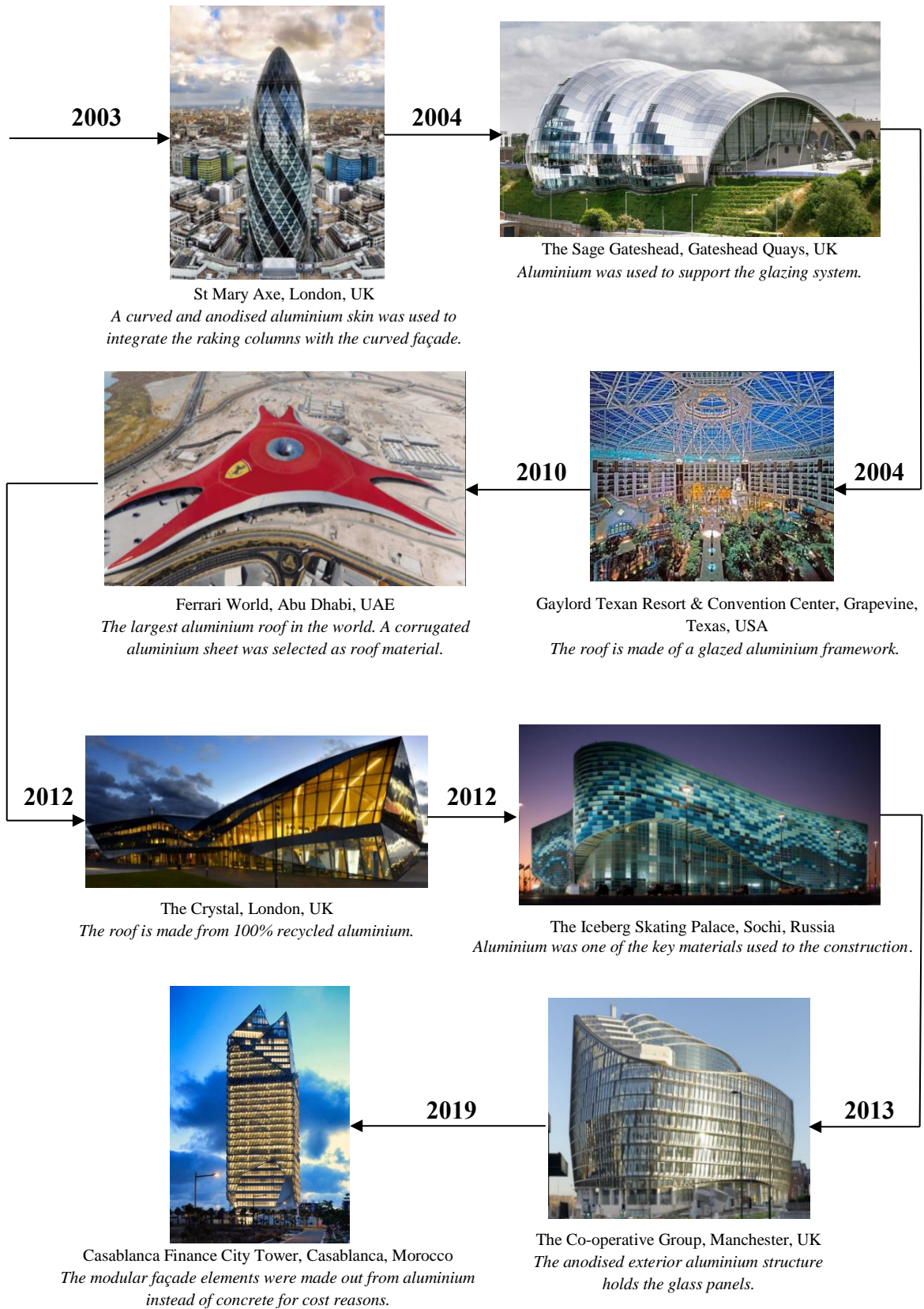*The anodised exterior aluminium structure holds the glass panels.*

Figure 1: Examples of aluminium alloy structures.

The purpose of this paper is to provide a comprehensive review of the experimental, numerical and analytical research work to date on the structural performance and design of aluminium alloy structures. Upon a brief introduction in Section 1, the material properties of aluminium alloys are discussed in Section 2. In Sections 3, 4 and 5, studies focussing on the structural performance of columns, beams and beam-columns are presented, respectively. Reported works on residual stresses and web crippling of aluminium sections are summarised in Sections 6 and 7. Studies on aluminium-concrete composite structures are outlined in Section 8. Reported research on connections is presented in Section 9. Section 10 reviews experimental and numerical works on other aluminium structural elements. Finally, concluding remarks on the overall investigation accompanied by suggestions for future work are presented in Section 11.

2   Material properties

2.1. Overview of aluminium alloy grades

Aluminium alloys are divided into two basic categories: wrought and cast alloys. The former comprises alloys which are melted in a furnace and then poured into moulds, whereas the latter includes alloys treated in a solid form. Depending on the strengthening working conditions aluminium alloys can be classified as heat-treatable and not heat-treatable. The Aluminum Association Inc. classifies the wrought alloys into 9 series using a four-digit system and each series comprises different combinations of alloying additions [2]. The first digit ($\underline{X}$xxx) indicates the principal constituent alloy, whereas the second digit (x$\underline{X}$xx) indicates the modifications made in the original alloy. The last two digits (xx$\underline{XX}$) are arbitrary numbers so that the specific alloy can be identified in the series. Thus, the material properties can vary offering several options for applications. Research on aluminium alloys in terms of their structural response has focussed on wrought alloys and particularly on 5xxx and 6xxx series that are the most attractive for structural engineering applications due to their mechanical properties [8-10]. The alloy classification is also followed by the temper designation in order to provide more information about the fabrication treatment. The temper designation consists of five basic tempers; F, O, H, W, or T, accompanied by additional digits for more details about the fabrication treatment, as described in Table 2.

Table 2: Summary of basic tempers for wrought alloys and the corresponding subdivisions (adapted from [9]).

Basic tempers for wrought alloys		Subdivisions of basic tempers
F (fabricated)	The thermal conditions during working or strain-hardening process to obtain specific material properties do not demand any special control.	-
O (annealed)	Treatment under high-temperature conditions in order to achieve maximum workability, toughness and ductility.	-
H (strain-hardened)	Used for non-heat-treatable alloys cold worked by strain-hardening method in order to stabilise their strength.	The first digit indicates the type of the thermal treatment and the second the amount of strain-hardening.
W (solution heat treated)	Applied to alloys subjected to natural aging after the solution heat treatment. Rather limited designation.	-
T (thermally treated)	Used for heat-treatable alloys subjected to natural or artificial aging in order stable tempers different than F, O, or H to be elaborated.	The first digit indicates the main type of heat treatment and the second to fifth [if they exist] the amount of stress release and other special treatments.

2.2. Material properties under monotonic loading

A series of tensile coupon tests have been conducted in a wide spectrum of aluminium alloys available in the market, aiming to investigate their material properties. Typical engineering stress-strain curves of commonly investigated structural aluminium alloys are presented in Figure 2 and typical mechanical properties are summarised in Table 3. In this table, E is the Young's Modulus, $f_{0.2}$ is the stress at 0.2% strain (also known as proof stress), f_u is the ultimate stress and n is the hardening exponent according to Ramberg – Osgood constitutive model [11]. A stress-strain curve of conventional structural carbon steel [12] is also included in Figure 2 for comparison purposes. As it can be seen in Figure 2, the stress-strain relationship of the aluminium alloys is characterised by a rounded curve without a distinct yielding point contrary to carbon steel. The initial material behaviour is linear elastic and is defined to relatively low stress, $f_{0.01}$, that corresponds to strain of 0.01%. After this point the material exhibits non-linear elastic behaviour up to $f_{0.2}$ stress, whilst beyond this point, plastic strains occur. Note that the $f_{0.2}$ or proof stress constitutes a threshold after which the stress-strain curve presents a "knee" followed by a strain-hardening branch. On the other hand, carbon steel behaves similarly at the elastic range but with larger and stiffer slope, followed by a clearly defined yield plateau and strain-hardening branch. Comparing the stress-strain curves from different aluminium series in Figure 2, it is apparent that 7xxx series have higher yield stress, but lower ductility compared to 6xxx series. It can also be seen from Table 3 that more pronounced ductility is observed for 6063-T5 and 6082-T4 and more evident strain-hardening is exhibited by 6082-T4 with $f_{0.2}/f_u$ equal to 0.54. The yield and tensile strengths of additional commonly used structural aluminium grades are presented for reference in Figure 3, where $f_{0.2}$ and f_u have been reported in the range of 80 to 275 MPa and 160 to 350 MPa, respectively [5].
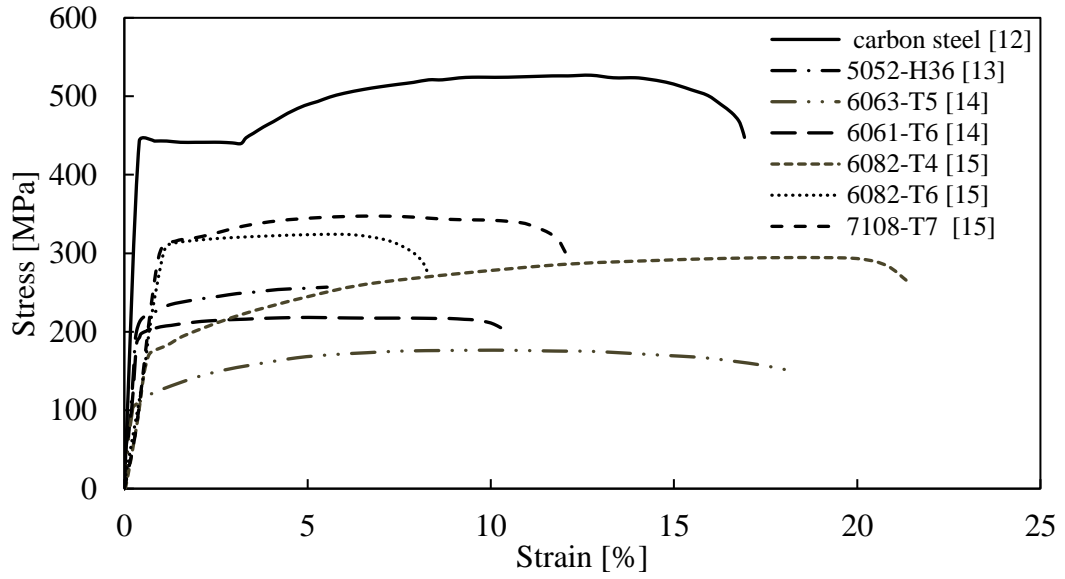
Figure 2: Stress-strain curves from corresponding tensile coupon tests [12-15].

Table 3: Mechanical properties of commonly investigated aluminium alloys.

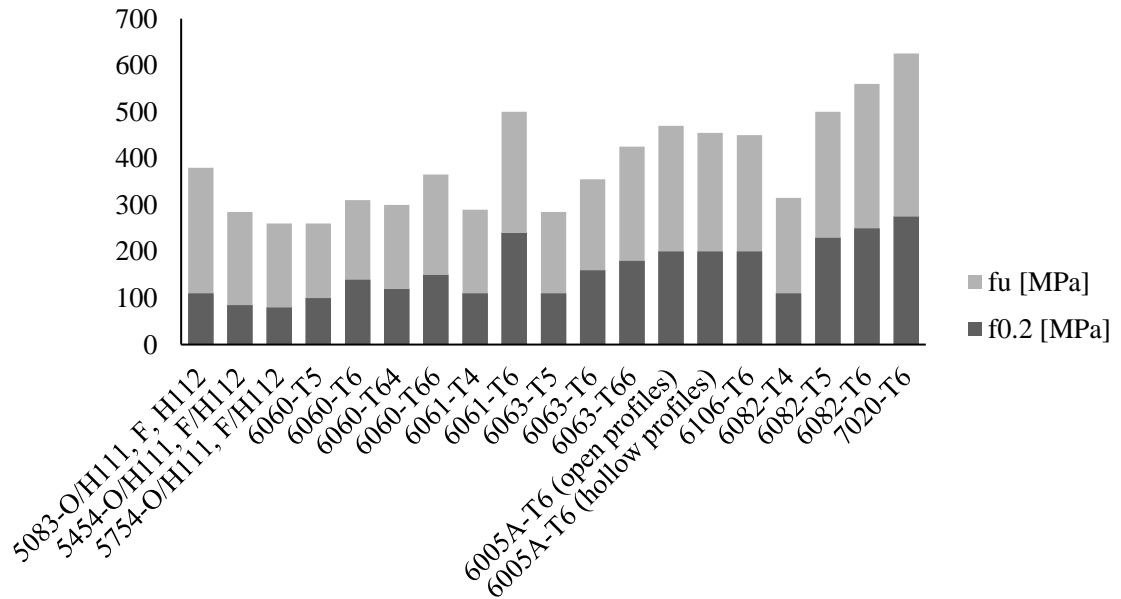| Author(s) (date) [Reference]	Aluminium grade	$f_{0.2}$ [MPa]	f_u [MPa]	E [GPa]	$f_{0.2}/f_u$	n
Alsanat et al. (2019) [13]	5052-H36	211.6	257.8	64.2	0.82	-
Su et al. (2014) [14]	6061-T6	234.0	248.0	66.0	0.94	12
Su et al. (2014) [14]	6063-T5	179.0	220.0	69.0	0.81	10
Moen et al. (1999) [15]	6082-T4	120.1	221.0	66.9	0.54	26
Moen et al. (1999) [15]	6082-T6	312.2	324.2	66.7	0.96	74
Moen et al. (1999) [15]	7108-T7	314.0	333.4	66.9	0.94	65

Figure 3: Yield and tensile strengths of commonly used aluminium grades.

In order to simulate the stress-strain response of aluminium alloys, the Ramberg-Osgood model [11] can be applied. Further to this, Baehre [16] proposed a satisfactory analytical approach, but was unable to capture the observed "knee" of the experimental stress-strain curves. De Matteis et al. [17] modified Baehre's law on the basis of experimental evidence improving its suitability. Guo et al. [18] investigated the material properties of 6061-T6 aluminium alloy and found that the stress-strain relationship derived from the Ramberg-Osgood model [11] combined with the Steinhardt Suggestion [19] allowed precise capture of its mechanical behaviour. It is noteworthy that the Steinhardt Suggestion [19] greatly simplifies the description of the constitutive relationship as it determines the hardening exponent n without considering the 0.1% stress ($f_{0.1}$). Wang et al. [20] performed a series of tensile coupon tests on 6082-T6 aluminium alloys and proposed a constitutive model based on the Ramberg-Osgood law, combined with the application of the fast-simulated annealing method for the calculation of n.

2.3. Material properties under cyclic loading

The ductility and energy dissipation of structural materials are of great significance for the response of structural members subjected to seismic loading. As can be seen in Table 4, there is lack of reported works on the cyclic behaviour of aluminium alloys, which sets limitations on their usage in earthquake prone areas. Early attempts to obtain an understanding of the hysteretic behaviour of aluminium alloys date back to 1990s. Hopperstad et al. [21] performed uniaxial cycling tests on specimens made from 6060 in tempers T4 and T5 under constant and varying strain amplitudes. They suggested an amendment to the cyclic plasticity model of Chaboche [22], so that the Bauschinger effect of temper T4 is precisely considered. Aiming to further investigate T4 aluminium alloys, the same authors conducted biaxial proportional and non-proportional cycling tests and extended the previous constitutive model to capture the observed influence of the strain range and the strain path shape on the material hardening [23]. The aforementioned tests could not clarify the presence of hardening behaviour, due to the low strain amplitudes (<2%) during the cyclic tests. To this end, Dusicka & Tinker [24] investigated the hysteretic response of coupons generated by 6061-T6/511 alloys subjected to constant strain amplitudes beyond 2%. The observed slight increase of the cyclic softening behaviour indicated its potential for seismic retrofit applications. De Matteis et al. [17] conducted cyclic tests on coupons of an almost pure aluminium alloy coded 1050A-H24 and found that it has substantial dissipative capacity largely for higher applied strain levels. More recently, Guo et al. [25] proposed a new constitutive model for the hysteretic behaviour of 6082-T6 and 7020-T6 on the basis of the monotonic curve and the reduction factor method. Based on the above, more cyclic tests are suggested to be performed to cover a wider range of aluminium alloys available in the market.

Table 4: Summary of tests on material properties of aluminium alloys under cyclic loading.
(in chronological order from most recent research)

Author(s) (date) [Reference]	Aluminium grade	Strain range [%]
Guo et al. (2018) [25]	6082-T6, 7020-T6	up to 4
Dusicka & Tinker (2013) [24]	6061-T6/511	2-4
De Matteis et al. (2012) [17]	1050A-H24	-
Hopperstand et al. (1995) [21,23]	6060-T4, 6060-T5	up to 1.2

2.4. Material properties of Heat-Affected Zone

A noteworthy characteristic of aluminium is that when high strength heat-treated aluminium alloys (6xxx series) are welded in order to be joined with adjacent structural members, the strength in the vicinity of the welded region is decreased significantly. This is an important demerit of these particular aluminium alloys which cannot be neglected during the design. The inferior material properties of this localised region around the welds, known as Heat-Affected Zone (HAZ), are considered through the application of softening factors. According to AA 2020 [7], the HAZ extends about 25.4 mm around the weld. The influence of the HAZ on the structural behaviour of beams and columns was demonstrated by Lai & Nethercot [26] using numerical analysis. Mazzolani [27] determined that the parent metal strength can be reduced almost 50% due to the presence of HAZ in 6xxx series aluminium alloys, whereas Zhu & Young [28] found that the proof stress can undergo a decrease up to 70%.

2.5. Material properties at elevated temperatures

Since 1990s a remarkable amount of studies on the material properties of aluminium alloys under fire conditions has been reported. Kaufman [29] significantly contributed to this research field by conducting steady state tests on 158 different aluminium alloys and found that the Young's Modulus (E) is independent of the heating rate. Langhelle [30] and Hepples & Wale [31] investigated the structural response of 6082 subjected to steady state thermal conditions. Faggiano et al. [32] emphasised on the way that elevated temperatures affect the material hardening factor and proposed a modified stress-strain relationship based on the Ramberg-Osgood expression. Maljaars et al. [33] performed tests on 5083-O/H111 and 6060-T66 and modified the Dorn-Harmathy creep model [34,35] so that to be applicable for 6xxx series aluminium alloys. Furthermore, Kandare et al. [36] modified the Larson-Miller model [37] on the basis of fire tests on coupons formed by 5083-H116. The reported test results were used for the assessment of a thermo-mechanical model developed by Kandare et al. [38] as well as an advanced modelling approach for fire conditions proposed by Feih et al. [39]. More recently, Chen et al. [40] investigated experimentally the post-fire behaviour of 6061-T6 and 7075-T73 and suggested simplified design formulae. Su & Young [41] presented a series of empirical equations regarding the mechanical properties of 6063-T5 and 6061-T6 exposed to fire. In the same study, design specifications were assessed, showing that the present partial factors lead to conservative design predictions. This is shown in Figure 4, where the test results from both steady and transient tests appear far from the EN 1992-1-2 [42] design curve. The studies, also, concluded that the behaviour under fire conditions is complex and dependent on the chemical

composition of each aluminium alloy. Additional tests that will allow more accurate design models for each aluminium alloy ensuring both economy and safety are necessary.
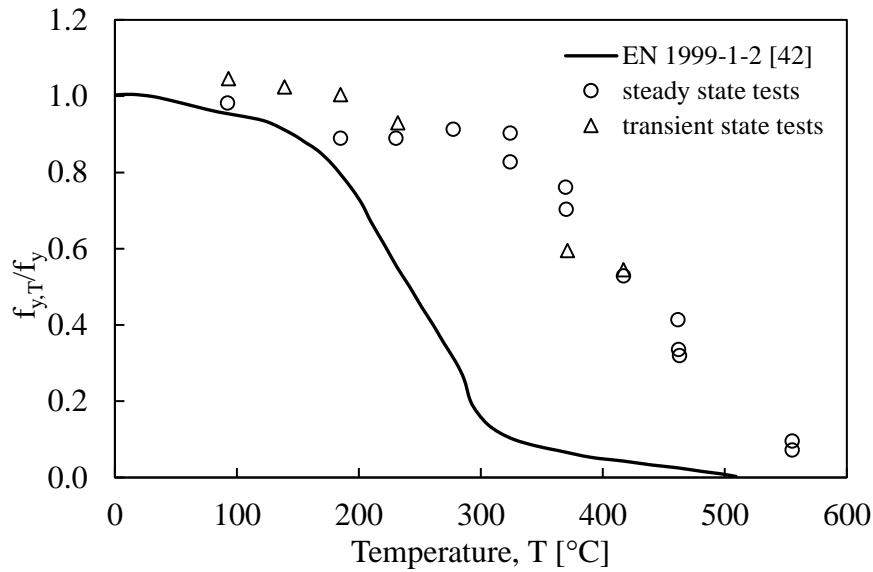

Figure 4: Comparison between test results and EN 1999-1-2 [42] predictions (adapted from [41]).

3   Columns

3.1. Local buckling

The design resistance of an aluminium structural member under compression is governed by the cross-section classification. This is a codified procedure that implicitly treats local buckling phenomenon, i.e. the buckling of the constituent plate elements of a cross-section under compression. EN 1999-1-1 [5] classifies the cross-sections in four classes, using cross-section slenderness limits (dependent on the boundary conditions of the constituent plate elements of a cross-section), the plate element stress distribution and the heat-treatment method. Classes 1, 2 and 3 comprise cross-sections capable of yielding without failing due to local buckling, while in Class 4 sections local buckling occurs in the elastic range and thus a reduced cross-sectional area is considered for the evaluation of the cross-sectional resistance.

Aiming to study local buckling and the cross-sectional performance, early tests on stub columns have been reported [43-47]. More recently, a considerable amount of stub column tests have been conducted in a wide range of cross-sectional shapes (Figure 5), aluminium grades and width-to-thickness ratios of the most slender constituent plate element. Zhu et al. [48] investigated the behaviour of plain and lipped channel (C-) stub columns, whereas Mazzolani et al. [49] tested angles and proposed an empirical equation about the local buckling resistance. Liu et al. [50,51] studied the local buckling behaviour of stiffened and irregular-shaped cross-sections and Yuan et al. [52] evaluated experimentally the post-buckling behaviour of slender (i.e. large width to thickness ratio) I-sections. Wang et al. [53] conducted stub columns tests on CHSs made from 6082-T6, whilst Feng & Young [54] dealt with perforated cross-sections. Following, Feng et al. [55,56] determined the reduced load-bearing capacity due to the presence

of holes by testing perforated stub columns with rectangular hollow sections (RHSs), square hollow sections (SHSs) and circular hollow sections (CHSs). Upon experimental testing on tubular sections, Su et al. [14] highlighted the significant contribution of the material strain-hardening on the cross-section capacity and assessed the applicability of the Continuous Strength Method (CSM) [57,58], that was originally developed for stainless steel stocky (i.e. small width to thickness ratio) cross-sections. Su et al. [59,60] extended the CSM to cover aluminium sections and proposed new slenderness limits as well as an effective thickness formula on the basis of collected data.

The studies are listed in Table 5, where the design code assessment is also shown. The mean values and coefficient of variation (COV) of ratios of the reported test strength, N_u, to the code predicted strength, N_{pred}, are included. For mean ratios N_u/N_{pred} higher than unity, the predictions are conservative, for lower than unity they are unsafe and for close to unity they are accurate. Furthermore, high values of COV suggest scattering and thus the predictions are considered as unreliable. As it can be seen, excessively conservative predictions were reported for channel sections in [48], which is opposed to an economic design process. In general, only a few studies indicated accurate cross-sectional strength predictions. The lack of accuracy is also related to the fact that the design formulae for aluminium often adopt similar principles to structural steel design, without sufficient consideration of the differences between the two materials. Modifications in line with obtained test data on aluminium are needed.
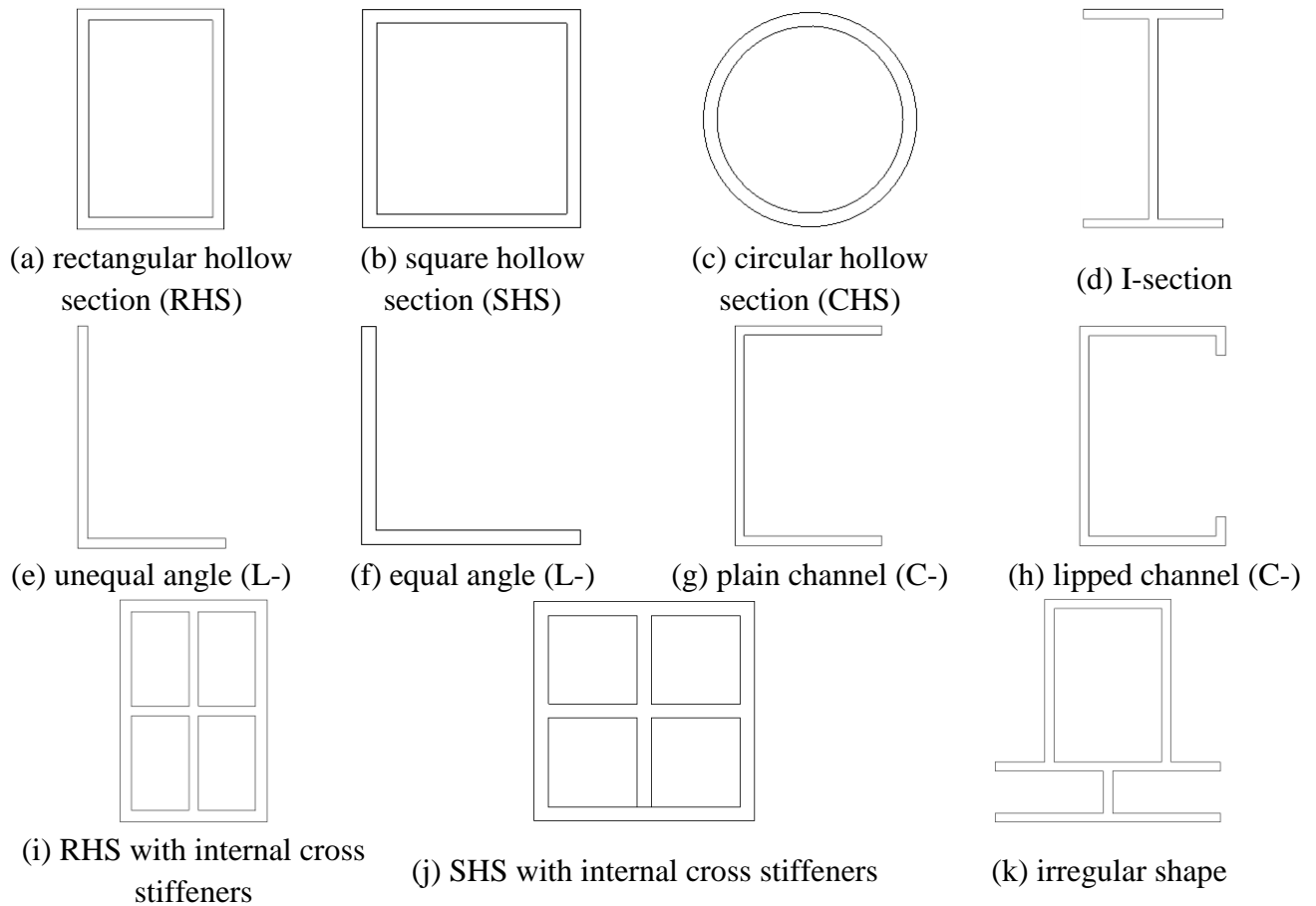

(a) rectangular hollow section (RHS) (b) square hollow section (SHS) (c) circular hollow section (CHS) (d) I-section

(e) unequal angle (L-) (f) equal angle (L-) (g) plain channel (C-) (h) lipped channel (C-)

(i) RHS with internal cross stiffeners (j) SHS with internal cross stiffeners (k) irregular shape

Figure 5: Cross-sectional shapes employed in stub column investigations.

Table 5: Summary of aluminium alloy stub column tests.
(in chronological order from most recent research)

Author(s) (date) [Reference]	Aluminium grade	Shape	No of tests	Width-to-thickness ratios	Design codes	N_u/N_{pred} mean	COV	Assessment
Zhu et al. (2019) [48]	6063-T5, 6061-T6	plain C-, lipped C-	8	25.50-25.90	GB 50429-2007 [4]	1.65	0.06	conservative
					EN 1999-1-1:2007 [5]	1.35	0.07	conservative
					AS/NZS 1664.1:1997 [6]	1.28	0.15	conservative
					AA [7]	1.28	0.15	conservative
					NAS [125]	1.21	0.10	conservative
					CSM [59,60]	1.12	0.16	conservative
Feng et al. (2018) [55]	6063-T5, 6061-T6	perforated RHS, SHS	16	27.30-43.67	NAS [125]	0.92	0.11	unsafe
Feng et al. (2016) [56]	6063-T5, 6061-T6	perforated CHS	10	23.48-49.81	NAS [125]	1.50	0.11	conservative
Wang et al. (2015) [53]	6082-T6	CHS	9	14.00-26.70	-			
Feng & Young (2015) [54]	6061-T6	perforated SHS	28	6.20-48.30	AISI 2008 [121]	0.96	0.32	unsafe
					NAS [125]	0.95	0.33	unsafe
Yuan et al. (2015) [52]	6061-T6, 6063-T5	I-	15	35.70-71.70	GB 50429-2007 [4]	1.13	0.12	conservative
					EN 1999-1-1:2007 [5]	1.12	0.12	conservative
					AS/NZS 1664.1:1997 [6]	1.10	0.09	conservative
					AA [7]	1.06	0.09	conservative
Liu et al. (2015) [51]	6063-T5	irregular	7	-	-			
Liu et al. (2015) [50]	6063-T5	stiffened closed-sections	10	-	GB 50429-2007 [4]	0.96	0.05	accurate
					EN 1999-1-1:2007 [5]	1.01	0.04	accurate
					AA [7]	0.94	0.08	unsafe
					DSM [65]	0.83	0.04	unsafe
					AISI 2008 [121]	0.98	0.08	accurate
Su et al. (2014) [14]	6061-T6, 6063-T5	SHS, RHS (with and without internal stiffeners)	15	3.20-20.70	EN 1999-1-1:2007 [5]	1.07	0.09	conservative
					AS/NZS 1664.1:1997 [6]	1.34	0.16	conservative
					AA [7]	1.19	0.16	conservative
					CSM [59,60]	1.04	0.06	accurate
Mazzolani et al. (2011) [49]	6xxx	angles	64	2.90-35.40[*]	-			

[*]calculated according to available data.

3.2. Flexural buckling

The flexural buckling behaviour of aluminium alloy columns has been under thorough investigation, being one of the primary constituents for the assurance of the structural integrity. According to the current design guidelines, buckling classes are determined by two material groups based on the temper designation, as shown in Table 6.

Table 6: Material groups based on temper designation. (adapted from Wang et al. [53])

Specifications	Material group 1	Material group 2
GB 50429-2007 [4]	T6	Other tempers
EN 1999-1-1:2007 [5]	T6, H14/24/34	Other tempers
AS/NZS 1664.1:1997 [6]	T5, T6, T7, T8, T9	O, H, T1, T2, T3, T4
AA 2020 [7]	T5, T6, T7, T8, T9	O, H, T1, T2, T3, T4
Note: Material groups 1 and 2 refer to buckling curves A and B in EC9, respectively.		

In order to comprehend the ultimate performance of aluminium alloy columns, early studies have been reported by Hopperstad et al. [45] who tested 6082-T4 and 6082-T6 columns, and Manevich [61] who numerically investigated the influence of the material strain-hardening on the critical buckling stress. Over the last years, a considerable amount of experimental studies has been performed, as summarised in Table 7. In this table, the test boundary conditions and the slenderness ratio, L_e/r, of the specimens are also included (L_e is the effective buckling length and r the radius of gyration of the cross-section). Wang et al. [53] focussed on the reliability level of current design rules on CHSs columns, while Adeoti et al. [62] expanded the investigation on columns formed by H-sections and RHSs. Wang et al. [63] studied L-shaped columns manufactured by 7A04 high-strength aluminium alloy, whereas Wang et al. [64] focussed on I-section columns. Feng et al. [56] investigated the buckling behaviour of perforated columns, suggesting that a properly modified Direct Strength Method (DSM) [65], a design approach suggested for cold-formed steel sections, could be suitable for the design of CHS columns with circular openings. After two years, Feng et al. [55] reported that the DSM cannot be applied for the design of perforated RHS and SHS columns. The aforementioned test results were also used by Feng & Liu [66] to conduct an extensive parametric study and adjust the EN 1999-1-1 [5] equations, taking into account the reduced cross-sectional area due to perforation. A numerical study on irregular-shaped sections was carried out by Chang et al. [67] who concluded that the DSM is able to predict the interactive buckling failure mode accurately but not in every case. Recently, Wang et al. [68] tested columns with large RHS and I- sections and Zhu et al. [48,69] presented their test results on plain and lipped channel columns. As shown in Table 7, the reported test data have been used to assess current design rules and it can be concluded that the international guidelines are overly conservative and confirm the need for further research into this field. In addition, many of past studies have focussed on hollow sections, which are less prone to torsional failure. Hence, despite the exhaustive experimental and numerical investigation on the structural response of columns, test data on interactive torsional-flexural buckling behaviour are relatively limited and further research is recommended.

Table 7: Summary of aluminium alloy column experiments.
(in chronological order from most recent research)

Author(s) (date) [Reference]	Aluminium grade	Shape	No of tests	Boundary conditions	Slenderness ratio [L_e/r]	Design codes	N_u/N_{pred} mean	COV	Assessment
Zhu et al. (2019) [48]	6063-T5, 6061-T6	plain C-, lipped C-	20	fixed ends	-	GB 50429-2007 [4]	1.38	0.20	conservative
						EN 1999-1-1:2007 [5]	1.45	0.14	conservative
						AS/NZS 1664.1:1997 [6]	1.23	0.16	conservative
						AA [7]	1.23	0.16	conservative
						NAS [125]	1.21	0.15	conservative
Wang et al. (2018) [68]	6061-T6	I-, RHS	7	pinned ends	28.96-116.74	GB 50429-2007 [4]	1.55	0.25	conservative
						EN 1999-1-1:2007 [5]	1.30	0.22	conservative
						AA [7]	1.06	0.19	conservative
Feng et al. (2018) [55]	6063-T5, 6061-T6	perforated RHS, SHS	21	pinned ends	13.94-93.22	NAS [125]	0.97	0.07	accurate
Wang et al. (2017) [64]	6063-T5, 6061-T6	I-	11	fixed-pinned ends	46.90-67.50	GB 50429-2007 [4]	1.45	0.13	conservative
						EN 1999-1-1:2007 [5]	1.45	0.11	conservative
						AS/NZS 1664.1:1997 [6]	1.27	0.09	conservative
						AA [7]	1.13	0.13	conservative
Feng et al. (2016) [56]	6063-T5, 6061-T6	perforated CHS	8	pinned ends	28.84-58.88	NAS [125]	1.27	0.12	conservative
Wang et al. (2016) [63]	7A04	L-	42	pinned ends	15.00-100.00	GB 50429-2007 [4]	2.76	0.27	conservative
						EN 1999-1-1:2007 [5]	1.21	0.21	conservative
						AA [7]	1.19	0.34	conservative
Adeoti et al. (2015) [62]	6082-T6	H-, RHS	30	pinned ends	22.36-163.01	GB 50429-2007 [4]	1.14	0.09	conservative
						EN 1999-1-1:2007 [5]	1.14	0.09	conservative
						AA [7]	1.20	0.09	conservative
						GB 50017-2003 [103]	1.21	0.10	conservative
Wang et al. (2015) [53]	6082-T6	CHS	15	pinned ends	24.42-73.99*	EN 1999-1-1:2007 [5]	1.10	0.08	conservative
						AS/NZS 1664.1:1997 [6]	0.97	0.13	accurate
						AA [7]	1.14	0.13	conservative

*calculated according to available data.

3.3. Welded columns

As mentioned in Section 2.4, the reduced strength of the HAZ affects the structural response of the structural member and thus it should be considered during the design process. To this end, Zhu & Young [28,70-74] examined the buckling behaviour of RHSs, SHSs and CHSs columns with and without transverse welds. They proposed new design criteria for the ultimate strength based on the DSM and new values for HAZ softening factors. Zhu et al. [75] extended this investigation to channel sections and modified the DSM and the CSM approach to make them applicable to welded channel columns. Feng et al. [55] dealt with perforated RHS and SHS columns incorporating welded and non-welded specimens. Their experimental outcomes demonstrated the applicability of the design criteria proposed by Zhu & Young [72] to welded columns.

3.4. Columns at elevated temperatures

In order to comprehend the buckling response and design of columns at elevated temperatures, experimental and numerical work has been performed, as listed in Tables 8 and 9, respectively. Langhelle & Amdahl [76] performed column buckling tests to clarify the consequences of the viscoplastic behaviour at elevated temperatures. Suzuki et al. [77] conducted a series of column

tests under fire conditions and extended the simple plastic theory to estimate the critical temperature beyond which column failure occurs. Maljaars et al. [78,79] carried out axial compression tests and finite element (FE) analyses on slender SHSs and angles under steady and transient state conditions and proposed new less conservative cross-section classification limits for EN 1999-1-2 [42]. In a following numerical work, Maljaars et al. [80,81] pointed out that the stress-strain relationships at elevated temperatures are more curved than at ambient temperature and that the buckling resistance is directly linked to the inelastic critical stress. Liu et al. [82] determined the buckling behaviour of columns with irregular-shaped cross sections by numerical means and suggested a modification to the equations provided by EN 1999-1-2 [42]. In a more recent study, Jiang et al. [83] performed tests and FE models on RHS and CHS columns and modified the stability coefficient of EN 1999-1-1 [5] and GB 50429 [4] to take into account the effect of the elevated temperatures on the normalised slenderness and the imperfection parameter.

Table 8: Summary of tests on columns at elevated temperatures.
(in chronological order from most recent research)

Author(s) (date) [Reference]	Type of test	Aluminium grade	Shape	No of tests	Temperature [°C]	Design codes	Assessment
Jiang et al. (2018) [83]	axial compression	6061-T66	RHS, CHS	108	up to 400	-	
Maljaars et al. (2009) [78]	axial compression	5083-H11, 6060-T66	SHS, L-	55	up to 330	EN 1999-1-2 [42]	conservative
Suzuki et al. (2005) [77]	fire resistance test [loaded and non-loaded heating]	5083-O, 5083-H112	box, H-	23	up to 850	-	
Langhelle & Amdahl (2001) [76]	axial compression	6082	-	31	-	-	

Table 9: Summary of numerical investigations on columns at elevated temperatures.
(in chronological order from most recent research)

Author(s) (date) [Reference]	Type of test	Aluminium grade	Shape	No of analyses	Temperature [°C]	Design codes	Assessment
Jiang et al. (2018) [83]	axial compression	6063-T5, 6061-T6, 6063-T6, 6061-T4	RHS, CHS, J-, T-, L-, C-, Z-, T- [one sym. axis]	8829	up to 400°C	-	
Liu et al. (2016) [82]	axial compression	6061-T6	irregular shaped	300	up to 500°C	GB 50429-2007 [4] EN 1999-1-1:2007 [5] EN 1999-1-2 [42] AA [7] DSM [65] AISI 2008 [121]	conservative conservative conservative conservative conservative conservative
Maljaars et al. (2009) [79,80,81]	axial compression	5083-O/H111, 6060-T66	SHS, I-	48	200,300	EN 1999-1-2 [42]	conservative

4 Beams

4.1. Flexural resistance

The flexural resistance and rotational capacity of beams are of significant importance in order to ensure the safe transfer of the vertical loads to the foundation. This is one of the earliest research topics, since the first experimental works date back to 1950s, when Panlilo [84] investigated the behaviour of two-span statically indeterminate beams. Later, Mazzolani et al. [85] extended the plastic design to aluminium alloy structures and Welo [86] performed tests under uniform moment and determined the moment-curvature behaviour. Thereon, numerous experimental and numerical investigations have been carried out on aluminium beams under 3-, 4- and 5-point bending conditions, as summarised in Table 10. Opheim [87] conducted 4-point bending tests and found that there is no significant difference between tensile and compressive behaviour of 6060-T4 beams. Moen et al. [15,88] demonstrated through experimental and numerical studies that the rotational capacity is dependent on the material strain-hardening and the magnitude of the moment gradient. Their test results [15] were used by De Matteis et al. [89] who proposed new limits on the cross-section classification of EN 1999-1-1 [5], considering the material strain-hardening. The importance of the material strain-hardening was also highlighted by Su et al. [90-93]. In another study, Zhu & Young [94] modified the current DSM achieving more accurate and reliable design provisions for flexural SHS members. Kim & Peköz [95] developed a new formulation for the stress at ultimate limit state based on test results of doubly symmetric I-section beams. Kim & Peköz [96] also presented a simplified design approach named Numerical Slenderness Approach in order to determine the nominal stresses of each constituent plate element of a complex section under flexure. The reliability of the proposed method was evaluated by performing a series of tests on beams with mullion sections. Castaldo et al. [97] numerically studied the ultimate behaviour of RHS beams under non-uniform bending and proposed multivariate non-linear equations for their ultimate flexural

resistance and rotational capacity. Piluso et al. [98] extended the aforementioned study to I-sections fabricated by 6082-T4 and 6063-T5. Experimental and numerical studies on perforated CHS beams subjected to gradient and constant moments were reported by Feng et al. [99,100]. They found that the presence of holes, their size and number reduce the flexural capacity. Recently, Montuori et al. [101] reported a thorough finite element investigation on I-beams formed by high-yielding low-hardening aluminium alloys. The outcomes denoted that the increased values of slenderness parameter and shear length ratio reduce the rotational capacity. Focussing on lateral-torsional buckling, Cheng et al. [102] investigated numerically the lateral stability of I-section beams and suggested a modification to the GB 50017-2003 [103]. The proposed modified design methodology was assessed by Wang et al. [104] concluding that it provides more accurate predictions compared to EN 1999-1-1 [5]. A few years later, Wang et al. [105] extended their investigation conducting experiments on I-beams including specimens with and without intermediate stiffeners subjected to concentrated loads.

Table 10 summarises the studies and the design code assessment by providing the mean and COV values of the reported obtained ultimate flexural strengths (M_u) over design strengths predicted by the international design codes (M_{pred}). The overall high M_u/M_{pred} ratios reveal largely conservative design estimations. The latter can also be visualised in Figure 6, which presents reported M_u values normalised by M_{pred} of EN 1999-1-1 [5], and plotted against the cross-sectional slenderness parameter (b/t, i.e. width to thickness ratio). In addition, as shown in Table 10, there are only a few reported studies on 5-point bending tests and hence additional experiments are suggested to better evaluate the plastic performance of indeterminate beams.

Table 10: Summary of investigations on beams.
(in chronological order from most recent research)

Author(s) (date) [Reference]	Type of study	Aluminium grade	Type of bending test	Shape	No of tests	Design codes	M_u/M_{pred} mean	COV	Assessment
Montuori et al. (2020) [101]	FE	6061-T6, 6082-T6	3-point	H-, I-	240	-			
Feng et al. (2020) [100]	Exp	6061-T6, 6063-T5	3-point, 4-point	perforated CHS	8	NAS [125]	1.20	0.23	conservative
Feng et al. (2019) [99]	FE	6061-T6, 6063-T5	3-point, 4-point	perforated CHS	408	-			
Piluso et al. (2019) [98]	FE	6082-T4, 6063 T5	3-point	H-, I-	240	-			
Kim & Peköz (2018) [96]	Exp & FE	6063-T5	4-point	mullion	2 & -	AA [7]			conservative
Castaldo et al.(2017) [97]	FE	6082-T6	3-point	RHS	252	-			
Wang et al. [105]	Exp & FE	6061-T6, 6063-T5	simply supported	I-	10 & 24	EN 1999-1-1:2007 [5]	1.40	0.10	conservative
Su et al. (2016) [93]	Exp & FE	6063-T5, 6063-T6	3-point, 4-point, 5-point	SHS, RHS with internal stiffeners	30 & 150	EN 1999-1-1:2007 [5]	1.41	0.11	conservative
						AS/NZS 1664.1:1997 [6]	2.11	0.21	conservative
						AA [7]	1.67	0.18	conservative
						CSM [59,60]	1.30	0.10	conservative

| Reference	Method	Alloy	Loading	Section	Number	Design standard	Mean	COV	Assessment
Su et al. (2015) [91,92]	Exp& FE	6061-T6, 6063-T5	5-point	SHS, RHS	27& 120	EN 1999-1-1:2007 [5]	1.82	0.23	conservative
						AS/NZS 1664.1:1997 [6]	2.26	0.23	conservative
						AA [7]	2.02	0.26	conservative
						CSM [59,60]	1.39	0.16	conservative
Su et al. (2014) [90]	Exp & FE	6061-T6, 6063-T5	3-point, 4-point	SHS, RHS	29 & 132	EN 1999-1-1:2007 [5]	1.17	0.11	conservative
						AS/NZS 1664.1:1997 [6]	1.54	0.16	conservative
						AA [7]	1.38	0.14	conservative
						CSM [59,60]	1.11	0.11	accurate
Wang et al. (2012) [104]	Exp	6061-T6, 6063-T5	simply supported	I-	40	EN 1999-1-1:2007 [5]	0.92	0.13	unsafe
Kim & Peköz (2010) [95]	Exp & FE	6063-T6	4-point	I-	3 & -	AA [7]	1.21	0.06	conservative
Zhu & Young (2009) [94]	Exp & FE	6061-T6, 6063-T5	4-point	SHS	10 & 60	EN 1999-1-1:2007 [5]	1.31	0.11	conservative
						AS/NZS 1664.1:1997 [6]	1.38	0.20	conservative
						AA [7]	1.35	0.20	conservative
						DSM [65]	1.21	0.07	conservative
Cheng et al. (2006) [102]	FE	-	simply supported	I-	250	-			
De Matteis et al. (2001) [89]	FE	6082-T4, 6082-T6	4-point	RHS	-	EN 1999-1-1 [5]			conservative
Moen et al. (1999) [88]	FE	6082-T4, 6082-T6, 7108-T7	4-point	unwelded I-, welded I-, box	19	-			
Moen et al. (1999) [15]	FE	6082-T4, 6082-T6, 7108-T7	4-point	unwelded I-, welded I-, box	38	EN 1999-1-1 [5]	1.15	0.11	conservative
Opheim (1996) [87]	Exp & FE	6060-T4, 6064-T6	4-point	SHS	-	-			

17
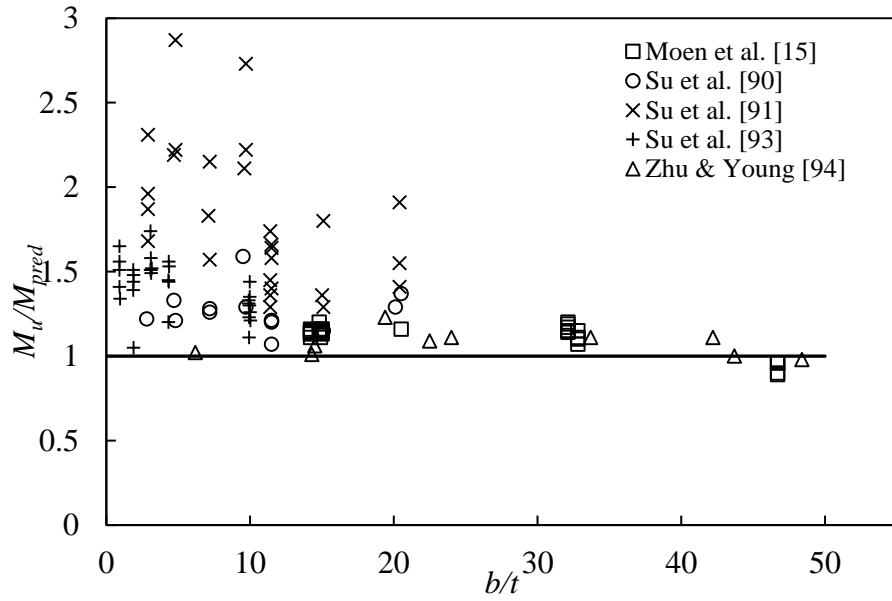
Figure 6: Comparison between test results and design predictions using EN 1999-1-1[5].

4.2. Welded beams

Until now relatively little attention has been given at the behaviour of aluminium alloy welded beams. Thus, the existing design approaches adopt the same principles to the corresponding ones for steel welded beams, leading to gross approximations, since the two materials differ considerably. Moen et al. [15,88] and Matusiak [106] presented their studies on welded I-beams highlighting the significant reduction on rotational capacity due to welding. The reported results by the latter were used by Wang et al. [107] who focussed on the vicinity of the weld and determined its impact on the total strength and ductility of the beams. The authors proposed a new modelling methodology for the region around the weld, assuming shell elements, geometric imperfections, plastic anisotropy, inhomogeneous material properties and ductile failure. The actual structural performance of welded beams is still ambiguous and thus more experimental research needs to be carried out.

4.3. Beams at elevated temperatures

A few studies have been carried out on the structural behaviour of beams exposed to fire. Suzuki et al. [77] performed fire resistance tests and proposed fire design formulae, whereas more recently, Meulen et al. [108] performed 3-point bending steady and transient state tests up to 300°C in order to assess the EN 1999-1-2 [42]. The experimental and numerical studies on aluminium beams at elevated temperatures are limited and thus more 3-, 4- and 5- point bending tests on different cross-sectional shapes in a wide range of applied strain rates are necessary. Data from these experiments will form a database that can be used for the development of more accurate design models and more reliable design provisions for aluminium alloys.

# 5	Beam-columns

The behaviour of aluminium alloy members under combined compression and bending has also been reported. Clark [109], Klöppel & Bärsch [110] and Gilson & Cescotto [111] performed tests on RHS, I- and T stocky sections. Zhu & Young [112,113] presented their experimental work on SHS, RHS and CHS specimens under combined axial compression and bending about the weak axis. The obtained outcomes demonstrated that the predicted beam-column strengths are underestimated by the current design guidelines. Zhao et al. [114-116] reviewed the Chinese Standards and proposed new values for certain design parameters. Furthermore, Zhu et al. [117] tested eccentrically compressed I-shaped members under elevated temperatures and presented a simplified correlation curve able to predict the bearing capacity of columns subjected to eccentric compression up to 300°C.

# 6	Residual stresses

The residual stresses developed during the manufacturing process can have a significant impact on the overall structural response of a member. According to Mazzolani [10], the residual stresses are quite low for extruded profiles, heat treated or not, and thus can be ignored, contrary to welded profiles, where the residual stresses can have a significant impact on the load-bearing capacity of the structure. Aiming for a better understanding of the residual stress distribution in aluminium sections, Huynh et al. [118] investigated the residual stresses of cold-rolled aluminium channel sections using the sectioning method. It was shown that the in-plane residual stresses were significant only in the corner parts of the smallest and thinnest C-section, whereas the out-of-plane residual stresses were considerable (up to 30% of yield stress) for all the investigated sections. Similar findings for cold-formed steel open sections have been reported by Moen et al. [119] and Gardner & Cruise [120]. There is a need to extend this investigation in various cold-formed, hot-rolled and welded cross-sections, so that the effect of residual stresses will be adequately considered in the design process.

# 7	Web crippling

Web crippling is specified as localised buckling and yielding of the web in the vicinity of the applied concentrated load. Research works examining the web crippling of a plethora of sections including end-two-flange (ETF), interior-two-flange (ITF), end-one-flange (EOF) and interior-one-flange (IOF) loading and boundary conditions, as defined in AISI 2008 [121], have been reported and summarised in Table 11. The first reported work was presented by Tryland et al. [122] who found that the web thickness and the flange stiffness considerably affects the ultimate capacity. Later Zhou & Young [123,124] conducted an extensive investigation on SHSs and RHSs in a wide slenderness range and suggested modified design formulae to the North American Specification (NAS) [125]. Zhou et al. [126] tested SHSs under concentrated bearing loads and proposed threshold slenderness values beyond which the web buckling becomes the predominant failure mode. Zhou & Young [127] extended their investigation on SHSs with perforated webs proposing a strength reduction factor and a new web crippling design equation for SHSs with circular web holes. Chen et al. [128] studied further the web

crippling behaviour of SHSs proposing new equations for the ultimate capacity. In another study, Su & Young [129] proposed a more accurate and reliable design methodology for the web bearing capacity of stocky sections which takes into account the significant effect of the material strain-hardening. Alsanat et al. [13,130] tested for first time roll-formed aluminium lipped channel sections under ETF and ITF conditions and proposed modified rules on the basis of the obtained test data. Recently, Zhou & Young [131] carried out tests on plain and lipped channel sections with restrained flanges. The assessment of the design specifications based on the most crucial loading-boundary condition are also summarised in Table 11, revealing the current lack of accuracy and reliability in the design predictions of the web crippling phenomenon. Contrary to the cross-sectional (Table 5), column (Table 9) and flexural strengths (Table 10) that are generally underestimated by the codes, Table 11 shows that overall the codified capacities against web crippling are not safely estimated.

Table 11: Summary of web crippling tests.
(in chronological order from most recent research)

Author(s) (date) [Reference]	Aluminium grade	Shape	No of tests	Loading-boundary conditions	Web slenderness ratios (b/t)	Design codes	N_u/N_{pred}		Assessment
							mean	COV	
Zhou & Young (2020) [131]	6063-T5, 6061-T6	lipped C-, plain C-	52	ETF, ITF	43.00-58.00	EN 1999-1-1:2007 [5]	0.75	0.26 (ETF)	unsafe
							1.18	0.32 (ITF)	
						AS/NZS 1664.1:1997 [6]	1.00	0.47 (ETF)	conservative
							1.06	0.28 (ITF)	
						AA [7]	1.00	0.47 (ETF)	conservative
							1.06	0.28 (ITF)	
						NAS [125]	1.12	0.36 (ETF)	unsafe
							0.62	0.40 (ITF)	
Alsanat et al. (2019) [13]	5052-H36	lipped C-	40	ETF, ITF	3.33-10.00*	AS/NZS 1664.1:1997 [6]	0.50	0.37 (ETF)	unsafe
							0.88	0.24 (ITF)	
						EN 1993-1-3:2005 [132]	0.49	0.06 (ETF)	unsafe
							0.60	0.07 (ITF)	
Su & Young (2018) [129]	6063-T5, 6061-T6	SHS, RHS	34	ETF, ITF, EOF, IOF	2.80-28.00	EN 1999-1-1:2007 [5]	0.53	0.23 (EOF)	unsafe
							0.78	0.19 (IOF)	
							0.87	0.14 (ETF)	
							1.16	0.11 (ITF)	
						AS/NZS 1664.1:1997 [6]	0.62	0.32 (EOF)	unsafe
							0.78	0.30 (IOF)	
							0.96	0.14 (ETF)	
							1.00	0.16 (ITF)	
						AA [7]	0.47	0.20 (EOF)	unsafe
							0.78	0.30 (IOF)	
							0.96	0.14 (ETF)	
							1.00	0.16 (ITF)	
						EN 1993-1-3:2005 [132]	3.14	0.31 (EOF)	conservative
							1.01	0.21 (IOF)	
							5.05	0.30 (ETF)	
							8.04	0.24 (ITF)	
						AISC [133]	0.54	0.25 (EOF)	unsafe
							0.88	0.22 (IOF)	
							0.87	0.12 (ETF)	
							1.19	0.12 (ITF)	
	-	SHS	48		30.00-88.00		2.45	0.53 (EOF)	conservative

Reference	Alloy	Section	No.	Loading	Thickness range	Design standard	Mean	COV	Assessment
Chen et al. (2015) [128]				ETF, ITF, EOF, IOF		EN 1993-1-3:2005 [132]	1.47	0.33 (IOF)	
							2.26	0.52 (ETF)	
							1.34	0.33 (IOF)	
						GB 50017 [103]	0.29	0.54 (EOF)	unsafe
							0.42	0.39 (IOF)	
							0.28	0.53 (ETF)	
							0.38	0.44 (IOF)	
Zhou & Young (2010) [127]	6061-T6	perforated SHS	84	ETF, ITF	6.20-49.50	EN 1999-1-1:2007 [5]	0.75	0.23 (ETF)	unsafe
							0.95	0.15 (ITF)	
						AA [7]	0.95	0.47 (ETF)	accurate
							0.97	0.29 (ITF)	
Zhou et al. (2009) [126]	6061-T6	SHS	64	ETF, ITF	6.20-48.30	EN 1999-1-1:2007 [5]	1.04	0.25 (EL)	accurate
							1.05	0.20 (IL)	
						AA [7]	1.86	0.37 (EL)	conservative
							1.46	0.25 (IL)	
Zhou & Young (2008) [123]	6063-T5, 6061-T6	SHS, RHS	150	EF[**], IF[***]	6.30-74.50	-			
Tryland et al. (1999) [122]	6082-T6	SHS, I-	52	-	-	-			

[*]calculated according to available data.
[**]EF: End-bearing Loading
[***]IL: Interior-bearing Loading

8 Composite structures

8.1. Aluminium-concrete structural members

Following similar concept and principles with the composite steel-concrete structures and in particular with the concrete-filled steel tubes (CFST), the possibility of combining aluminium with concrete has been investigated. Research work on the structural response of concrete-filled aluminium tubes (CFAT) with typical cross-sections shown in Figure 7 has been reported.
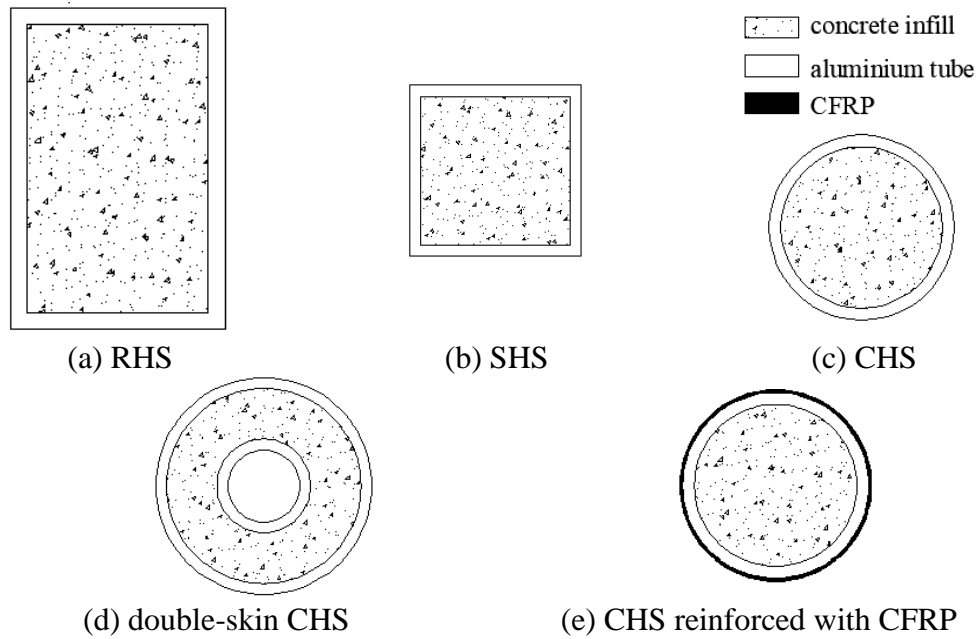

concrete infill
aluminium tube
CFRP

(a) RHS   (b) SHS   (c) CHS

(d) double-skin CHS   (e) CHS reinforced with CFRP

Figure 7: Investigated cross-sections of aluminium-concrete composite members [134-142].

Zhou & Young [134] conducted axial compression tests on concrete-filled aluminium stub columns with SHSs and RHSs and concluded that the AS/NZS 1664.1:1997 [6] and AA [7] design codes are generally unconservative. Later, Zhou & Young [135,136] extended their experimental investigation on CHS stub columns filled with concrete and developed design criteria considering the observed material interaction. In a more recent study, Zhou & Young [137] assessed experimentally the compressive response of concrete-filled double-skin tubes and suggested formulae for their ultimate capacity. Wang et al. [138] used the data reported by Zhou & Young [135] and evaluated whether the "nominal yield strength" method adopted by GB 50936 [139] for CFST is applicable to CFAT, concluding that it provides conservative but reliable predictions.

Feng et al. [140] tested simply-supported concrete-filled SHS and RHS beams, whereas Chen et al. [141] performed 4-point bending tests on concrete-filled CHS beams. In both investigations, the ultimate strength almost doubled thanks to the concrete infill, which prevented premature failure due to local buckling. Chen et al. [142] investigated the flexural behaviour of concrete-filled CHSs strengthened by carbon fibre-reinforced polymer (CFRP). It was observed that the slightly improved ultimate capacity was accompanied by a reduction in

the ductility. Modifications on the Architectural Institute of Japan (AIJ) standards [143] so as to consider the contribution of the CFRP reinforcement were also presented.

More research on this field should be carried out in order to adequately determine the structural behaviour of CFATs and propose design criteria able to achieve efficient exploitation of both materials. Future studies could include flexural buckling tests on CFATs with and without CFRP strengthening, beam-column tests, stub columns under eccentric compression and investigation of their behaviour at elevated temperatures.

8.2. Aluminium-CFRP structural members

Wu et al. [144] were at the forefront of strengthening aluminium alloy tubular sections against web crippling using CFRP, finding that the web crippling capacity can experience almost a four-fold increase due to the CFRP. Islam & Young [145] focussed on the effect of the application of six different types of adhesives and fibre-reinforced polymers (FRPs) on the web crippling capacity of SHSs and RHSs. It was shown that the higher the web slenderness ratio, the greater the enhancement of the web crippling strength. This was confirmed at their following experimental work [146] and the reported results were used in a recent numerical study where the NAS [125] design equations were modified in order to consider the contribution of both the CFRP-strengthening and the adhesive to the web crippling capacity [147].

9 Connections and joints

9.1. Welded

Owing to the difficulties related to the weldability of aluminium [148], only limited work has been reported to date on aluminium welded connections. Early attempts for a comprehensive understanding of the behaviour of welded connections were made by Soetens [149], who investigated experimentally and numerically the structural response of welded connections in RHSs fabricated by 6063-T5 and 7020-T6. His findings were incorporated in the international specifications for the design of aluminium alloy structures (ECCS [150], NEN 3854 [151], CP 118 [152]). Another research study on welded connections was performed by Chan & Porter Goff [153] who evaluated experimentally the effects of the reduced strength zone on the ultimate capacity, ductility and failure mode of 7xxx series aluminium alloys. The structural response of welded T-stub joints under monotonic tensile loading was examined by De Matteis et al. [154] and it was shown that EN 1999-1-1 [5] equations provide reliable although slightly underestimated design predictions. The scarcity of the reported data reveals the need of additional experiments on aluminium welded connections to enable a better understanding of their behaviour.

9.2. Bolted

Over the last two decades, a series of studies have been performed on bolted connections under various arrangements and load cases, as illustrated in Figure 8. Table 12 summarises the reported experimental work. De Matteis et al. [155,156] conducted a thorough experimental and numerical work on T-stub connections under monotonic and cyclic loading. Kim [157] carried out tests on single shear bolted connections and found that the curling effect (out-of-plane deformation) reduces suddenly the ultimate capacity. These findings were used by Cho & Kim [158] who modified the strength equations for block shear fracture and bearing factor, taking into account the curling effect. In a more recent study by Wang et al. [159], twenty bolted connections were tested under tensile loading and the obtained results were used for the assessment of GB 50429 [4], EN 1999-1-1 [5] and AA [7] design codes, concluding that the aforementioned design specifications lead to conservative predictions. De Matteis et al. [160] carried out an extensive parametric study on the structural behaviour of T-stub joints showing that the material strain-hardening and the ductility considerably affect the strength of the joint. Brando et al. [161] determined the ultimate capacity of the web in beam-to-column joints subjected to tension and adjusted the design criteria developed for steel joints by using correction factors that consider the mechanical characteristics of aluminium alloys. Recently, Adeoti et al. [162] reported a study dealing with the flexural behaviour of hexagonal bolted joints underling the importance of considering all the parameters with great impact on the structural behaviour and stiffness in order to design joints with high performance.
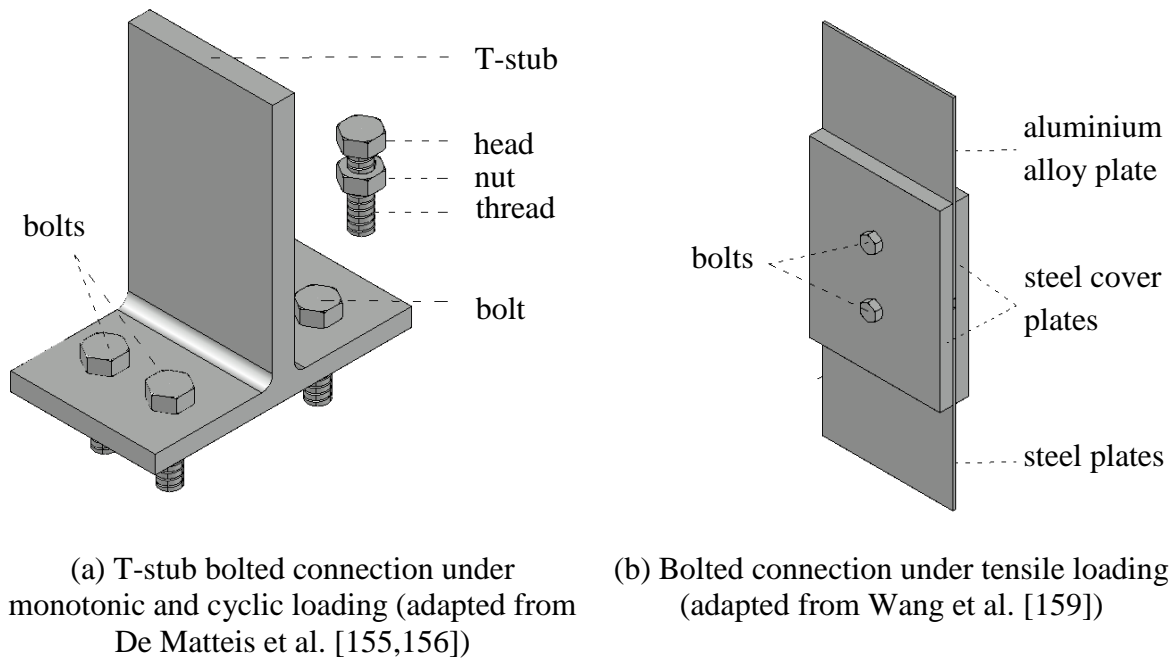

(a) T-stub bolted connection under monotonic and cyclic loading (adapted from De Matteis et al. [155,156])

(b) Bolted connection under tensile loading (adapted from Wang et al. [159])

Figure 8: Configuration of investigated bolted connections.

Table 12: Summary of aluminium alloy bolted connection/joint tests.
(in chronological order from most recent research)

Author(s) (date) [Reference]	Aluminium grade	Connection/joint type	No of tests	Design codes	N_u/N_{pred} mean	COV	Assessment
Adeoti et al. (2019) [162]	6082-T6	hexagonal bolted joints	6	-			
Wang et al. (2018) [159]	6061-T6, 6063-T5	shear connection in single shear with two bolts	20	EN 1999-1-1:2007 [5]	1.36	0.03	conservative
				AA [7]	1.42	0.11	conservative
				GB 50429-2007 [4]	2.78	0.12	conservative
Kim (2012) [157]	6061-T6	shear connection in single shear with four bolts	10	-			
De Matteis et al. (2004) [155]	6061-T6, 6082-T6, 7020-T6	welded plates with holes	26	-			

Over the last five years, there is also a wide usage of aluminium alloy gusset (AAG) pinned, rigid or semi-rigid joints in practice. Guo et al. [163,164] performed a series of tests on fourteen AAG joints in order to define their out-of-plane flexural response. The results were used to elaborate simplified design formulae about the resistance against block tearing and local buckling. Guo et al. [165] adapted the component method included in EN 1993-1-8 [166] for AAG steel joints system and proposed suitable expressions for their bending behaviour. Guo et al. [167] investigated the flexural response of AAG joints exposed up to 300°C and proposed design criteria for the bearing capacity and the non-linear flexural stiffness. In a further study by Guo et al. [168], the hysteretic behaviour of AAG joints was assessed through cycling loading tests. Shi et al. [169] conducted experiments on two-way AAG joints subjected to pure bending and shear loading and they proposed a theoretical model able to accurately capture the mechanical behaviour of these joint systems. Liu et al. [170] determined experimentally the flexural behaviour of double- and single- layer AAG joints. Comparisons between the two types of the investigated joints demonstrated the superior structural response of the former.

Additional research in order to obtain a better understanding of the structural response of bolted connections under various configurations, loading cases (static, cyclic and fatigue) and aluminium alloy types, is recommended. This will allow for design criteria able to take into account this complex behaviour and lead to safe and economic design solutions.

10   Other studies

Kesawan et al. [171] conducted experimental work on the flexural response of mullions caused by wind pressure and suction, whereas the following year a numerical study on long span mullions with complex-shape sections under wind suction was presented by them [172]. Scheperboer et al. [173] studied numerically the buckling behaviour of perforated steel and

aluminium plates and suggested that the design rules for steel perforated plates are applicable to aluminium alloy plates. Pursuing optimised cross-sectional shape with efficient exploitation of the material distribution, Tsavdaridis et al. [174] applied Structural Topology Optimization in aluminium cross-sections. They concluded that further research should be conducted including more global and local failure modes. Ampatzis et al. [175] suggested a useful methodology for determining the safety factor of spatial aluminium frame structures against elastoplastic collapse. He et al. [176] proposed a novel modular support structure assembled by a foldable plane frame and joints suitable for temporary structures. Finally, the hysteresis behaviour of aluminium shear panels has been investigated, demonstrating their potential as dissipative devices in seismic resistant structures [177-179]. Related to this, it is noteworthy that studies on the seismic behaviour of columns and beams remain scarce. Therefore, a series of tests on structural members subjected to cyclic loading would be an interesting future research field in terms of the investigation of their ductility and energy dissipation capacity.

11 Conclusions and future work

This paper reviewed the reported research work on structural aluminium alloys, providing a complete view of their mechanical properties, structural response and design of basic structural elements. The history of structural aluminium's investigation is relatively short and thus more research is needed in order to obtain a thorough understanding of its behaviour. On the basis of the reviewed papers, the following conclusions can be drawn:

1. Overall the current design guidelines do not provide accurate strength predictions, which are opposed to an economical and efficient design philosophy. This is related to the fact that their formulae are based on limited amount of experimental and numerical results. Design codes sometimes adopt similar principles to their steel structure counterparts, without sufficient consideration of the differences between the two materials.

2. Despite the advantageous features of structural aluminium alloys members, the investigation revealed that there are still limitations in their design, forcing the designers to favour more conventional materials.

3. Topics with limited number of studies that have been mentioned throughout this work are summarised in Table 13 as future recommendations. Additional research work can lead to modifications of the existing design codes and potentially increase structural engineers' confidence towards a more frequent employment of aluminium alloys.

4. Finally, scope of future work is to bridge the gap between theoretical and real world, making aluminium alloy an alternative construction material, capable of efficiently responding to the challenges encountered in real-life structures.

Table 13: Summary of recommended future work.

Investigation topic	Methods of investigation (experimental & numerical)
Material properties under cyclic loading	Cyclic tests coupons in a wide range of aluminium alloys.
Material properties at elevated temperatures	Coupon tests of various alloys under fire conditions in order to develop more accurate design models considering the chemical composition.
Interactive torsional-flexural buckling of columns	Column tests on open cross-sections of various aluminium alloys.
Flexural response	Bending tests on different cross-sectional shapes of welded beams. Inelastic performance of statically indeterminate beams
Flexural response at elevated temperatures	Bending tests including various cross-sectional shapes in a wide range of applied strain rates.
Influence of residual stresses on the structural performance	Measurements of magnitude and distribution of residual stresses in sections of various fabrication processes.
Structural response of concrete-aluminium elements	Structural members under various loading scenarios at room and elevated temperatures.
Structural response of connections	Welded and bolted connection tests under various configurations, loading cases (static, cyclic, fatigue) and aluminium alloy types.
Seismic behaviour of columns and beams	Cyclic tests to investigate ductility and energy dissipation capacity.

Acknowledgements

References

1. Aluminium in construction [Internet]. All about Aluminium. 2019 [accessed 1 June 2020]. Available from: https://aluminiumleader.com/application/construction/

2. Aluminum Alloys 101[Internet]. The Aluminum Association. 2019 [accessed 1 June 2020]. Avaliable from: https://www.aluminum.org/aluminum-sustainability

3. Aluminium-The Green Metal [Internet]. Hazlemere. 2020. [accessed 1 June 2020]. Available from: https://www.hazlemerecommercial.co.uk/blog/aluminium-the-green-metal/

4. GB 50429-2007. Code for design of aluminium structures. Ministry of Construction of the People's Republic of China.

5. Eurocode 9 (EC9): Design of aluminium structures. Part 1-1: General   structural rules - General structural rules and rules for buildings. BS EN 1999-1-1:2007, European Committee for Standarization (CEN):2007. BSI; 2007.

6. Australian/New Zealand Standard (AS/NZS) Aluminium structures part 1: Limit state design.AS/NZS 1664.1:1997. Standards Australia, Sydney, Australia. 1997.

7. The Aluminum Association. Aluminum Design Manual. Washington, D.C.; 2020.

8. Kaufman JG. Introduction to Aluminium Alloys and Tempers. ASM International. Materials Park, OH: ASM International; 2000.

9. Davis JR. Alloying: Understanding the Basics. Materials Park, OH: ASM International; 2001.

10. Mazzolani FM. Aluminium Structural Design. Vienna: Springer Verlag GmbH; 2003.

11. Ramberg W, Osgood WR. Description of stress-strain curves by three parameters. Vol. Technical. Washington, D.C.: National Advisory Committe for Aeronautics; 1943.

12. Foster ASJ, Gardner L, Wang Y. Practical strain-hardening material properties for use in deformation-based structural steel design. Thin-Walled Struct. 2015;92:115–29.

13. Alsanat H, Gunalan S, Guan H, Keerthan P, Bull J. Experimental study of aluminium lipped channel sections subjected to web crippling under two flange load cases. Thin-Walled Struct. 2019;141:460–76.

14. Su MN, Young B, Gardner L. Testing and Design of Aluminum Alloy Cross Sections in Compression. J Struct Eng. 2014;140(9).

15. Moen LA, Hopperstad OS, Langseth M. Rotational Capacity Of Aluminum Beams Under Moment Gradient. I: Experiments. J Struct Eng. 1999;125(8):910–20.

16. Baehre R. Trycktastravorav elastoplastikt material-nagrafragestallningar (Comparison between structural behaviour of elastoplastic material). Tekn Arne Johnson Ingenjorsbyra. 1966.

17. De Matteis G, Brando G, Mazzolani FM. Pure aluminium: An innovative material for structural applications in seismic engineering. Constr Build Mater. 2012;26(1):677–86.

18. Guo X, Shen Z, Li Y. Stress-strain relationship and physical-mechanical properties of domestic structural aluminum alloy. J Build Struct. 2007;06:110–7.

19. Steinhardt PJ, Nelson DR, Ronchetti M. Bond-orientational order in liquids and glasses. Phys Rev B. 1983;28:784–805.

20. Wang Y, Fan F, Qian H, Zhai X. Experimental study on constitutive model of high-strength aluminum alloy 6082–T6. J Build Struct. 2013;34(6):113–20.

21. Hopperstad OS, Langseth M, Remseth S. Cyclic stress-strain behaviour of alloy AA6060, Part I : Uniaxial experiments and modelling. Int J Plast. 1995;11(6):725–39.

22. Chaboche JL. Constitutive equations for cyclic plasticity. Int J Plast. 1989;5:247–302.

23. Hopperstad OS, Langseth M, Remseth S. Cyclic stress-strain behaviour of alloy AA6060 T4 , Part II : Biaxial experiments and modelling. Int J Plast. 1995;11(6):741–62.

24. Dusicka P, Tinker J. Global Restraint in Ultra-Lightweight Buckling-Restrained Braces. J Compos Constr. 2013;17(1):139–50.

25. Guo X, Wang L, Shen Z, Zou J, Liu L. Constitutive model of structural aluminum alloy under cyclic loading. Constr Build Mater. 2018;180:643–54.

26. Lai YFW, Nethercot DA. Strength of aluminium members containing local transverse welds. Eng Struct. 1992;14(4):241–54.

27. Mazzolani FM. Aluminum alloy structures. 2nd ed. London: E& FN Spon; 1995.

28. Zhu JH, Young B. Effects of transverse welds on aluminum alloy columns. Thin-Walled Struct. 2007;45(3):321–9.

29. Kaufman JG. Properties of Aluminum Alloys: Tensile, Creep, and Fatigue Data at High and Low Temperatures. ASM International; 1999.

30. Langhelle NK. Experimental validation and calibration of nonlinear finite element models for use in design of aluminium structures exposed to fire. Norwegian University of Science and Technology, Trondheim; 1999.

31. Hepples W, Wale D. High temperature tensile properties of 6082-T651. 1992.

32. Faggiano B, De Matteis G, Landolfo R, Mazzolani FM. Behaviour of aluminium alloy structures under fire. J Civ Eng Manag. Vilnius Gedminas Technical University; 2004;10:183–90.

33. Maljaars J, Soetens F, Katgerman L. Constitutive model for Aluminum alloys exposed to fire conditions. Metall Mater Trans A Phys Metall Mater Sci. 2008; 39A:778-789.

34. Dorn JE. Some Fundamental Experiments on High Temperature Creep. J Mech Phys Solids. 1954;3:85–116.

35. Harmathy TZ. A Comprehensive Creep Model. J Fluids Eng. 1967;89(3):496–502.

36. Kandare E, Feih S, Lattimer BY, Mouritz AP. Larson – Miller Failure Modeling of Aluminum in Fire. Metall Mater Trans A. 2010;41(12):3091–9.

37. Larson FR, Miller J. A Time-Temperature Relationship for Rupture and Creep Stresses. Trans ASME. 1952;74(5):765–75.

38. Kandare E, Feih S, Kootsookos A, Mathys Z, Lattimer BY, Mouritz AP. Creep-based life prediction modelling of aluminium in fire. Mater Sci Eng A. 2010;527(4–5):1185–93.

39. Feih S, Kandare E, Lattimer BY, Mouritz AP. Structural analysis of compression deformation and failure of aluminum in fire. J Struct Eng. 2011;137(7):728–38.

40. Chen Z, Lu J, Liu H, Liao X. Experimental investigation on the post-fire mechanical properties of structural aluminum alloys 6061-T6 and 7075-T73. Thin-Walled Struct. 2016;106:187–200.

41. Su MN, Young B. Material properties of normal and high strength aluminium alloys at elevated temperatures. Thin-Walled Struct. 2019;137:463–71.

42. Eurocode 9 (EC9) : Design of aluminium structures. Part 1-2: Structural fire design. BS EN 1999-1-2:2007, European Committee for Standarization (CEN):2007. BSI; 2010.

43. Mazzolani FM, Faella C, Piluso V, Rizzano G. Assessment of stub column tests for aluminium alloys. In: 2nd International Conference on Coupled Instabilities in Metal Structures, CIMS '96. Imperial College Press, London; 1996.

44. Langseth M, Hopperstad OS. Local buckling of square thin-walled aluminium extrusions. Thin-Walled Struct. 1997;27:117–26.

45. Hopperstad OS, Langseth M, Tryland T. Ultimate strength of aluminium alloy outstands in compression: experiments and simplified analysis. Thin-Walled Struct. 1999;34:279–94.

46. Mazzolani FM, Piluso V, Rizzano G. Experimental analysis of aluminium alloy channels subjected to local buckling under uniform compression. In: Italian Conference on Steel Construction. Milano, Italy; 2001.

47. Faella C, Mazzolani F, Piluso V, Rizzano G. Local Buckling of Aluminium Members: Testing and Classification. J Struct Eng. 2000;126(3):353–60.

48. Zhu JH, Wang P, Liu T. Numerical simulation and design of aluminum compression members with plain and lipped channel sections. J Build Struct. 2010;31:163–8.

49. Mazzolani FM, Piluso V, Rizzano G. Local Buckling of Aluminum Alloy Angles under Uniform Compression. J Struct Eng. 2011;137(2):173–84.

50. Liu M, Zhang L, Wang P, Chang Y. Buckling behaviors of section aluminum alloy columns under axial compression. Eng Struct. 2015;95:127–37.

51. Liu M, Zhang L, Wang P, Chang Y. Experimental investigation on local buckling behaviors of stiffened closed-section thin-walled aluminum alloy columns under compression. Thin-Walled Struct. 2015;94:188–98.

52. Yuan HX, Wang YQ, Chang T, Du XX, Bu YD, Shi YJ. Local buckling and postbuckling strength of extruded aluminium alloy stub columns with slender I-sections. Thin-Walled Struct. 2015;90:140–9.

53. Wang Y, Fan F, Lin S. Experimental investigation on the stability of aluminium alloy 6082 circular tubes in axial compression. Thin-Walled Struct. 2015;89:54–66.

54. Feng R, Young B. Experimental Investigation of Aluminum Alloy Stub Columns with Circular Openings. J Struct Eng. 2015;141(11):1–10.

55. Feng R, Zhu W, Wan H, Chen A, Chen Y. Tests of perforated aluminium alloy SHSs and RHSs under axial compression. Thin-Walled Struct. 2018;130:194–212.

56. Feng R, Mou X, Chen A, Ma Y. Tests of aluminium alloy CHS columns with circular openings. Thin-Walled Struct. 2016;109:113–31.

57. Gardner L, Ashraf M. Structural design for non-linear metallic materials. Eng Struct. 2006;28(6):926–34.

58. Ashraf M, Young B. Design formulations for non-welded and welded aluminium columns using Continuous Strength Method. Eng Struct. 2011;33(12):3197–207.

59. Su MN, Young B, Gardner L. The continuous strength method for the design of aluminium alloy structural elements. Eng Struct. 2016;122:338–48.

60. Su MN, Young B, Gardner L. Classification of aluminium alloy cross-sections. Eng Struct. 2017;141:29–40.

61. Manevich AIÃ. Effect of strain hardening on the buckling of structural members and design codes recommendations. Thin-Walled Struct. 2007;45:810–5.

62. Adeoti GO, Feng F, Wang Y, Zhai X. Structures Stability of 6082-T6 aluminium alloy columns with H-section and rectangular hollow sections. Thin-Walled Struct. 2015;89:1–16.

63. Wang YQ, Wang ZX, Hu XG, Han JK, Xing HJ. Experimental study and parametric analysis on the stability behavior of 7A04 high-strength aluminum alloy angle columns under axial compression. Thin-Walled Struct. 2016;108:305–20.

64. Wang YQ, Yuan HX, Chang T, Du XX, Yu M. Compressive buckling strength of extruded aluminium alloy I-section columns with fixed-pinned end conditions. Thin-Walled Struct. 2017;119:396–403.

65. Moen CD, Schafer BW. Direct strength method for design of cold-formed steel columns with holes. J Struct Eng. 2011;137(5):559–70.

66. Feng R, Liu J. Numerical investigation and design of perforated aluminium alloy SHS and RHS columns. Eng Struct. 2019;199.

67. Chang Y, Liu M, Wang P. Interacted buckling failure of thin-walled irregular-shaped aluminum alloy column under axial compression. Thin-Walled Struct. 2016;107:627–47.

68. Wang ZX, Wang YQ, Sojeong J, Ouyang YW. Experimental investigation and parametric analysis on overall buckling behavior of large-section aluminum alloy columns under axial compression. Thin-Walled Struct. 2018;122:585–96.

69. Zhu JH, Li ZQ, Su M-N, Young B. Behaviour of aluminium alloy plain and lipped channel columns. Thin-Walled Struct. 2019;135:306–16.

70. Zhu JH, Young B. Tests and Design of Aluminum Alloy Compression Members. J Struct Eng. 2006;132(7):1096–107.

71. Zhu JH, Young B. Aluminum alloy tubular columns-Part I: Finite element modeling and test verification. Thin-Walled Struct. 2006;44(9):961–8.

72. Zhu JH, Young B. Aluminum alloy tubular columns-Part II: Parametric study and design using direct strength method. Thin-Walled Struct. 2006;44(9):969–85.

73. Zhu JH, Young B. Experimental investigation of aluminum alloy circular hollow section columns. Eng Struct. 2006;28:207–15.

74. Zhu JH, Young B. Numerical investigation and design of aluminum alloy circular hollow section columns. Thin-Walled Struct. 2008;46:1437–49.

75. Zhu JH, Li ZQ, Su MN, Young B. Numerical study and design of aluminium alloy channel section columns with welds. Thin-Walled Struct Struct. 2019;139:139–50.

76. Langhelle NK, Amdahl Jø. Experimental And Numerical Analysis of Aluminium Columns Subjected to Fire. The Eleventh International Offshore and Polar Engineering Conference. Stavanger, Norway: International Society of Offshore and Polar Engineers; 2001.

77. Suzuki JI, Ohmiya Y, Wakamatsu T, Harada K. Evaluation of Fire Resistance of Aluminum Alloy Members. Fire Sci Technol. 2005;24(4):237–55.

78. Maljaars J, Soetens F, Snijder HH. Local buckling of aluminium structures exposed to fire. Part 1: Tests. Thin-Walled Struct. 2009;47(11):1404–17.

79. Maljaars J, Soetens F, Snijder HH. Local buckling of aluminium structures exposed to fire Part 2 : Finite element models. Thin-Walled Struct. 2009;47(11):1418–28.

80. Maljaars J, Twilt L, Soetens F. Flexural buckling of fire exposed aluminium columns. Fire Saf J. 2009;44(5):711–7.

81. Maljaars J, Soetens F, Snijder H. H. Local Buckling of Fire-Exposed Aluminum Members: New Design Model. J Struct Eng. 2010;136(1):66–75.

82. Liu M, Chang Y, Wang P, Zhang L. Buckling behaviors of thin-walled aluminum alloy column with irregular-shaped cross section under axial compression in a fire. Thin-Walled Struct. 2016;98:230–43.

83. Jiang S, Xiong Z, Guo X, He Z. Buckling behaviour of aluminium alloy columns under fire conditions. Thin Walled Struct. 2018;124(1239):523–37.

84. Panlilo F. The theory of limit design applied to magnesium alloy and aluminium alloy structures. R Aerinautical Soc. 1947;534–71.

85. Mazzolani FM, Capelli M, Spasiano G. Plastic analysis of aluminium alloy members in bending. Aluminium. 1985;61(10):734–41.

86. Welo T. Inelastic deformation capacity of flexurally-loaded aluminium alloy structures. Norwegian University of Science and Technolog; 1990.

87. Opheim BS. Bending of thin-walled aluminium extrusions. Norwegian University of Science and Technology; 1996.

88. Moen LA, De Matteis G, Hopperstad OS, Langseth M, Landolfo R. Rotational Capacity Of Aluminum Beams Under Moment Gradient. II: Numerical Simulations. J Struct Eng. 1999;125(8):921–9.

89. De Matteis G, Moen LA, Langseth M, Landolfo R, Hopperstad OS, Mazzolani FM. Cross-sectional classification for aluminum beams-parametric study. J Struct Eng. 2001;127(3):271–9.

90. Su MN, Young B, Gardner L. Deformation-based design of aluminium alloy beams. Eng Struct. 2014;80:339–49.

91. Su MN, Young B, Gardner L. Continuous beams of aluminum alloy tubular cross sections. I: Tests and FE model validation. J Struct Eng. 2015;141(9).

92. Su MN, Young B, Gardner L. Continuous beams of aluminum alloy tubular cross sections. II: Parametric study and design. J Struct Eng. 2015;141(9).

93. Su MN, Young B, Gardner L. Flexural response of aluminium alloy SHS and RHS with internal stiffeners. Eng Struct. 2016;121:170–80.

94. Zhu JH, Young B. Design of Aluminum Alloy Flexural Members Using Direct Strength Method. J Struct Eng. 2009;135(5):558–66.

95. Kim Y, Peköz T. Ultimate flexural strength of aluminum sections. Thin-Walled Struct. 2010;48:857–65.

96. Kim Y, Peköz T. Numerical Slenderness Approach for design of complex aluminum extrusions subjected to flexural loading. Thin-Walled Struct. 2018;127:62–75.

97. Castaldo P, Nastri E, Piluso V. Ultimate behaviour of RHS temper T6 aluminium alloy beams subjected to non-uniform bending: Parametric analysis. Thin-Walled Struct. 2017;115:129–41.

98. Piluso V, Pisapia A, Nastri E, Montuori R. Ultimate resistance and rotation capacity of low yielding high hardening aluminium alloy beams under non-uniform bending. Thin-Walled Struct. 2019;135:123–36.

99. Feng R, Shen C, Lin J. Finite element analysis and design of aluminium alloy CHSs with circular through-holes in bending. Thin-Walled Struct. 2019;144.

100. Feng R, Chen Z, Shen C, Roy K, Chen B, Lim JBP. Flexural capacity of perforated aluminium CHS tubes–An experimental study. Struct. 2020;25:463-480.

101. Montuori R, Nastri E, Piluso V, Pisapia A. Ultimate behaviour of high-yielding low-hardening aluminium alloy I-beams. Thin-Walled Struct. 2020;146.

102. Cheng M, Shi Y, Wang Y. Analysis of lateral stability of I-section aluminum beams. Sci China Ser E Technol Sci. 2006;49(6):742–51.

103. GB 50017-2003. Code of Design of Steel Structures. Beijing: China Planning Press. Beijing: China Planning Press; 2003.

104. Wang YQÃ, Yuan HX, Shi YJ, Cheng M. Lateral torsional buckling resistance of aluminium I-beams. Thin-Walled Struct. 2012;50(1):24–36.

105. Wang YQ, Wang ZX, Yin FX, Yang L, Shi YJ, Yin J. Experimental study and fi nite element analysis on the local buckling behavior of aluminium alloy beams under concentrated loads. Thin-Walled Struct. 2016;105:44–56.

106. Matusiak M. Strength and ductility of welded structures in aluminium alloys. Norwegian University of Science and Technology; 1999.

107. Wang T, Hopperstad OS, Lademo OG, Larsen PK. Finite element modelling of welded aluminium members subjected to four-point bending. Thin-Walled Struct. 2007;45(3):307–20.

108. Meulen OR, Soetens F, Maljaars J. Experimental Analysis of Stability of Aluminium Beams in Case of Fire. J Struct Fire Eng. 2014;5(2):161–74.

109. Clark JW. Eccentrically loaded aluminum columns. Trans ASCE. 1955;120(116):1116–32.

110. Klöppel K, Bärsch W. Versuche zum kapitel "stabilitätsfälle" der neufassung von din 4113. Aluminium. 1973;49(10).

111. Gilson S, Cescotto S. Experimental research on the buckling of aluminium alloy columns with unsymmetrical cross-section. Lab Mécanique des Mater Théorie des Struct Liege, Liege, Belgium. 1982.

112. Zhu JH, Young B. Experimental Investigation of Aluminum Alloy Thin-Walled Tubular Members in Combined Compression and Bending. J Struct Eng. 2006;132(12):1955–66.

113. Zhu JH, Young B. Aluminum alloy circular hollow section beam-columns. Thin-Walled Struct. 2006;44(2):131–40.

114. Zhao Y, Zhai X, Sun L. Test and design method for the buckling behaviors of 6082-T6 aluminum alloy columns with box-type and L-type sections under eccentric compression. Thin-Walled Struct. 2016;100:62–80.

115. Zhao Y, Zhai X, Wang J. Buckling behaviors and ultimate strengths of 6082-T6 aluminum alloy columns under eccentric compression – Part I : Experiments and finite element modeling. Thin-Walled Struct. 2019;143.

116. Zhao Y, Zhai X, Wang J. Buckling behaviors and ultimate strength of 6082-T6 aluminum alloy columns with square and circular hollow sections under eccentric compression – Part II: Parametric study, design provisions and reliability analysis. Thin-Walled Struct. 2019;143.

117. Zhu S, Guo X, Liu X, Jiang S. Bearing capacity of aluminum alloy members under eccentric compression at elevated temperatures. Thin-Walled Struct. 2018;127:574–87.

118. Huynh LAT, Pham CH, Rasmussen KJR. Mechanical properties and residual stresses in cold-rolled aluminium channel sections. Eng Struct. 2019;199.

119. Moen CD, Igusa T, Schafer BW. Prediction of residual stresses and strains in cold-formed steel members. Thin-Walled Struct. 2008;46(4):1274–89.

120. Gardner L, Cruise R. Modeling of residual stresses in structural stainless steel sections. J Struct Eng. 2009;135(1):42–53.

121. AISI. Standard Test Method for Determining the Web Crippling Strength of Cold-Formed Steel Beams (AISI S909). Washington, D.C.; 2008.

122. Tryland T, Langseth M, Hopperstad OS. Nonperfect aluminium beams subjected to concentrated loading. J Struct Eng. 1990;125:900–9.

123. Zhou F, Young B. Aluminum tubular sections subjected to web crippling-Part I:. Tests and finite element analysis. Thin-Walled Struct. 2008;46(4):339–51.

124. Zhou F, Young B. Aluminium tubular sections subjected to web crippling–Part II: Proposed design equations. Thin-Walled Struct. 2008;46(4):352–61.

125. NAS. North American Specification for the Design of Cold-Formed Steel Structural Members. American Iron and Steel Institute, Washington, DC. 2001.

126. Zhou F, Young B, Zhao X. Tests and Design of Aluminum Tubular Sections Subjected to Concentrated Tests and Design of Aluminum Tubular Sections Subjected. J Struct Eng ASCE. 2009;135(7):806–17.

127. Zhou F, Young B. Web crippling of aluminium tubes with perforated webs. Eng Struct. 2010;32(5):1397–410.

128. Chen Y, Chen X, Wang C. Aluminum tubular sections subjected to web crippling. Thin-Walled Struct. 2015;90:49–60.

129. Su MN, Young B. Design of aluminium alloy stocky hollow sections subjected to concentrated transverse loads. Thin-Walled Struct. 2018;124:546–57.

130. Alsanat H, Gunalan S, Keerthan P, Guan H. Web crippling behaviour and design of aluminium lipped channel sections under two fl ange loading conditions. Thin-Walled Struct. 2019;144.

131. Zhou F, Young B. Web crippling of aluminium alloy channel sections with flanges restrained. Thin-Walled Struct. 2020;148.

132. Eurocode 3 (EC3): Design of Steel Structures, Part 1-3: General Rules-Supplementary Rules for Cold-Formed Members and Sheeting. BS EN 1993-1-3:2005, European Committee for Standarization (CEN):2005. BSI. 2005.

133. American Institute of Steel Construction, AISC Committee. Specification for Structural Steel Buildings, Chicago, Illinois, 2010.

134. Zhou F, Young B. Tests of concrete-filled aluminum stub columns. Thin-Walled Struct. 2008;46(6):573–83.

135. Zhou F, Young B. Concrete-filled aluminum circular hollow section column tests. Thin-Walled Struct. 2009;47(11):1272–80.

136. Zhou F, Young B. Numerical analysis and design of concrete-filled aluminum circular hollow section columns. Thin-Walled Struct. 2012;50(1):45–55.

137. Zhou F, Young B. Concrete-filled double-skin aluminum circular hollow section stub columns. Thin-Walled Struct. 2018;133:141–52.

138. Wang FC, Zhao HY, Han LH. Analytical behavior of concrete- filled aluminum tubular stub columns under axial compression. Thin-Walled Struct. 2019;140:21–30.

139. GB 50936-2014. Technical code for concrete filled steel tubular structures. 2014.

140. Feng R, Chen Y, Gong W. Flexural behaviour of concrete-filled aluminium alloy thin-walled SHS and RHS tubes. Eng Struct. 2017;137:33–49.

141. Chen Y, Feng R, Gong W. Flexural behavior of concrete-filled aluminum alloy circular hollow section tubes. Constr Build Mater. 2018;165:173–86.

142. Chen Y, Feng R, Xu J. Flexural behaviour of CFRP strengthened concrete-filled aluminium alloy CHS tubes. Constr Build Mater. 2017;142:295–319.

143. Architectural Institute of Japan (AIJ). Recomendations for Design and Construction of Concrete Filled Steel Tubular Structures, Architectural Institute of Japan, Tokyo, Japan, 1997.

144. Wu C, Zhao XL, Duan WH. Design rules for web crippling of CFRP strengthened aluminium rectangular hollow sections. Thin-Walled Struct. 2011;49:1195–207.

145. Islam SMZ, Young B. FRP strengthened aluminium tubular sections subjected to web crippling. Thin-Walled Struct. 2011;49:1392–403.

146. Islam SMZ, Young B. Web crippling of aluminium tubular structural members strengthened by CFRP. Thin-Walled Struct. 2012;59:58–69.

147. Islam SMZ, Young B. Design of CFRP-strengthened aluminium alloy tubular sections subjected to web crippling. Thin-Walled Struct. 2018;124:605–21.

148. Praveen P, Yarlagadda PKDV. Meeting challenges in welding of aluminum alloys through pulse gas metal arc welding. J Mater Process Technol. 2005;164–165:1106–12.

149. Soetens F. Welded connections in aluminium alloy structures. Heron. 1987;32(1).

150. European Recommendations for aluminium alloy structures (ECCS). First Edit. 1978.

151. TGB-Aluminium, Technical Principles for the design of building structures, Aluminium structures, Netherlands Standard NEN 3854. 1983.

152. CP 118, The structural use of aluminium, British Standard Code of Practice (replaced by BS 8118). 1969.

153. Chan T, Porter Goff R. Welded aluminium alloy connections: test results and BS8118. Thin-Walled Struct. 2000;36(4):265–87.

154. De Matteis G, Brescia M, Formisano A, Mazzolani FM. Behaviour of welded aluminium T-stub joints under monotonic loading. Comput Struct. 2009;87(15–16):990–1002.

155. De Matteis G, Corte GD, Mandara A, Mazzolani FM. Experimental behaviour of aluminium t-stub connections. In: Connections in Steel Structures V. Amsterdam; 2004.

156. De Matteis G, Naqash MT, Brando G. Effective length of aluminium T-stub connections by parametric analysis. Eng Struct. 2012;41:548–61.

157. Kim TS. Block Shear strength of single shear four-bolted connections with aluminium alloys – experiment and design strength comparison. Appl Mech Mater. 2012;217–219:386–9.

158. Cho YH, Kim TS. Estimation of ultimate strength in single shear bolted connections with aluminum alloys (6061-T6). Thin-Walled Struct. 2016;101:43–57.

159. Wang ZX, Wang YQ, Zhang GX, Shi YJ. Tests and parametric analysis of aluminum alloy bolted joints of different material types. Constr Build Mater. 2018;185:589–99.

160. De Matteis G, Mandara A, Mazzolani FM. T-stub aluminium joints : influence of behavioural parameters. Comput Struct. 2000;78(1–3):311–27.

161. Brando G, Sarracco G, De Matteis G. Strength of an Aluminum Column Web in Tension. J Struct Eng. 2014;141(7).

162. Adeoti GO, Fan F, Huihuan MA, Shen S. Investigation of aluminium bolted joint (HBJ) system behavior. Thin-Walled Struct. 2019;144:106100.

163. Guo X, Xiong Z, Luo Y, Qiu L, Liu J. Experimental investigation on the semi-rigid behaviour of aluminium alloy gusset joints. Thin-Walled Struct. 2015;87:30–40.

164. Guo X, Xiong Z, Luo Y, Xu H, Liang S. Block tearing and local buckling of aluminum alloy gusset joint plates. J Struct Eng. 2016;20(2):820–31.

165. Guo X, Xiong Z, Luo Y, Qiu L, Huang W. Application of the Component Method to Aluminum Alloy Gusset Joints. Adv Struct Eng. 2015;18(11):1931–46.

166. Eurocode 3 (EC3): Design of Steel Structures, Part 1-8: Design of Joints. BS EN 1993-1-8:2005, European Committee for Standarization (CEN):2005. BSI. 2005.

167. Guo X, Zhu S, Liu X, Wang K. Study on out-of-plane flexural behavior of aluminum alloy gusset joints at elevated temperatures. Thin-Walled Struct. 2018;123:452–66.

168. Guo X, Zhu S, Liu X, Liu L. Experimental study on hysteretic behavior of aluminum alloy gusset joints. Thin-Walled Struct. 2018;131:883–901.

169. Shi M, Xiang P, Wu M. Experimental investigation on bending and shear performance of two-way aluminum alloy gusset joints. Thin-Walled Struct. 2018;122:124–36.

170. Liu H, Ying J, Meng Y, Chen Z. Flexural behavior of double- and single-layer aluminum alloy gusset-type joints. Thin-Walled Struct. 2019;144.

171. Kesawan S, Mahendran M, Baleshan B. Section moment capacity tests of complex-shaped aluminium mullions. Thin-Walled Struct. 2018;131:855–68.

172. Kesawan S, Mahendran M. Member moment capacity of complex-shaped aluminium mullions under wind suction loading. Thin-Walled Struct. 2019;144.

173. Scheperboer IC, Efthymiou E, Maljaars J. Local buckling of aluminium and steel plates with multiple holes. Thin-Walled Struct. 2016;99:132–41.

174. Tsavdaridis KD, Efthymiou E, Adugu A, Hughes JA, Grekavicius L. Application of structural topology optimisation in aluminium cross-sectional design. Thin-Walled Struct. 2019;139:372–88.

175. Ampatzis AT, Psomiadis VG, Efthymiou E. Plastic collapse of hardening spatial aluminium frames: A novel shakedown-based approach. Eng Struct. 2017;151:724–44.

176. He L, Liu C, Wu Z, Yuan J. Stability analysis of an aluminum alloy assembly column in a modular support structure. Thin-Walled Struct. 2019;135:548–59.

177. Formisano A, Lombardi L, Mazzolani FM. Perforated metal shear panels as bracing devices of seismic-resistant structures. J Constr Steel Res. 2016;126:37–49.

178. De Matteis G, Brando G, Mazzolani FM. Hysteretic behaviour of bracing-type pure aluminium shear panels by experimental tests. Earthquake engineering & structural dynamics. 2011; 40(10):1143–1162.

179. De Matteis G, Mazzolani FM, and Panico S. Pure aluminium shear panels as dissipative devices in moment-resisting steel frames. Earthquake engineering & structural dynamics. 2007; 36(7): 841–859.